

10-A085 864

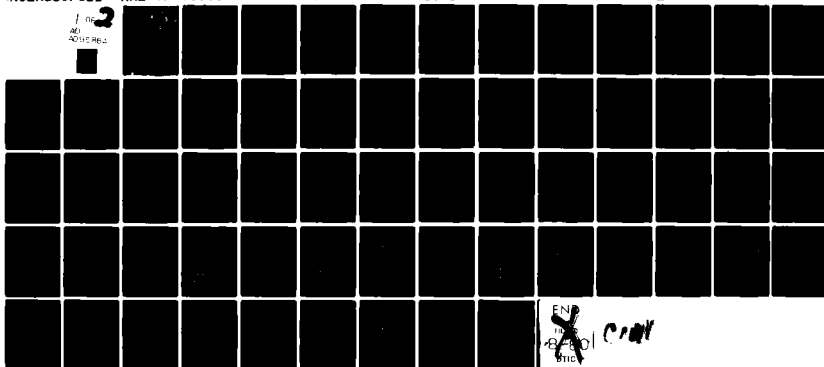
ROYAL AIRCRAFT ESTABLISHMENT FARNBOROUGH (ENGLAND) F/G 1/1  
ON THE USE IN STABILITY ANALYSIS OF THE RELATIONSHIPS BETWEEN T--ETC(U)  
JUN 79 H H THOMAS  
RAE-TR-79065

UNCLASSIFIED

DRIC-BR-70237

NL

10-A085 864



END  
IN  
B-101  
ETC

CAT

TR 79065

ADA 085864

DDC FILE COPY

DR70237

TR 79065

UNLIMITED



DTIC  
ELECT

FEB 28 1980

C

ROYAL AIRCRAFT ESTABLISHMENT

\***LEVEL**

Technical Report 79065

June 1979

**ON THE USE IN STABILITY ANALYSIS OF THE  
RELATIONSHIPS BETWEEN THE COEFFICIENTS  
OF A QUARTIC EQUATION AND THOSE OF  
A QUADRATIC FACTOR**

by

H.H.B.M. Thomas

\*

**Procurement Executive, Ministry of Defence  
Farnborough, Hants**

This document has been approved  
for public release and sale; its  
distribution is unlimited.

80 2 25 113

(18) DRIC

(19) BR-70237

UDC 533.6.013.4 : 512.393 : 517.912.2

(14) RAE-TR-79065

ROYAL AIRCRAFT ESTABLISHMENT

(9) Technical Report, 19065

Received for printing 7 June 1979

(6) ON THE USE IN STABILITY ANALYSIS OF THE RELATIONSHIPS BETWEEN THE COEFFICIENTS OF A QUARTIC EQUATION AND THOSE OF A QUADRATIC FACTOR. 1

by

(10) H. H. B. M. Thomas

(11) Jun 79

SUMMARY

(12) 63

The stability of the perturbed longitudinal motion of an unaugmented aircraft about a given trimmed flight condition is determined by the well-known stability quartic. It is shown that two basic relationships exist between the coefficients of the quartic and those of a quadratic factor. These relationships are linear in the coefficients of the quartic and the latter are in turn linear functions of the more important stability parameters. It is possible, therefore, to use the relationships, already mentioned, to derive a further equation connecting the two coefficients of the quadratic factor as a single stability parameter is varied, all others being held constant.

Examination of the position of the locus traced out by the point defined by the coefficients of the quadratic in relation to the axes and the parabolic boundary (separating real and complex roots) enables the trends in the nature of and the degree of stability of the mode or modes represented by the quadratic factor to be determined. Expressions are given which enable the value of the parameter being varied, and associated with a given point of the locus, to be calculated.

The use of this (as far as is known, novel) method of analysing aircraft stability is illustrated by a number of examples.

Departmental Reference: Aero 3456

Copyright

©

Controller, HMSO London  
1979

This document has been approved  
for public release and sale; its  
distribution is unlimited.

310450 Gm

# LIST OF CONTENTS

	<u>Page</u>
1 INTRODUCTION	3
2 RELATIONSHIP OF THE COEFFICIENT OF THE QUADRATIC FACTORS TO THOSE OF THE QUARTIC	4
3 RELATIONSHIP OF $g(G)$ TO $h(H)$ WHEN $m_u$ IS VARIED	8
3.1 Value of $g$ when $h = 0$	9
4 THE $g, h$ RELATIONSHIP FOR VARYING $m_w$	11
4.1 Value of $g$ for which $h = 0$	13
5 NUMERICAL EXAMPLE	13
6 VALUES OF THE PARAMETERS $m_u$ AND $m_w$ ASSOCIATED WITH POINTS OF THE $h, g$ CURVE	14
7 ANALYSIS IN TERMS OF THE PARAMETERS $K_n$ , STATIC MARGIN AND $H_m$ , MANOEUVRE MARGIN	15
8 DISCUSSION	17
9 CONCLUSIONS	18
Appendix A Analysis of the quartic in terms of the notation of R&M 2027	19
Appendix B Some remarks on the geometry of the locus of $g, h$	36
List of symbols	38
References	41
Illustrations	Figures 1-20
Report documentation page	inside back cover

Accession For	
NTIC	<input checked="" type="checkbox"/>
DDO TAB	<input type="checkbox"/>
Unannounced	<input type="checkbox"/>
Justification	
By	
Distribution	
Availability Codes	
Dist.	Avail and/or special
<i>M</i>	

## 1 INTRODUCTION

It is about a century ago since Routh<sup>1,2</sup> formulated his well-known necessary and sufficient conditions for the stability of a system as a set of inequalities to be satisfied by the coefficients of the characteristic or stability equation of the system. Since the earliest days of aviation use has been made of Routh's test functions (or their equivalents as given by Hurwitz<sup>3</sup> and independently by Frazer<sup>4,5</sup>) to ascertain the stability or otherwise of a given equilibrium motion of aeroplanes. However Routh's discriminant is a complicated expression even for the quartic stability equation, which results from the analysis of the simple case of the linearized motion of an aeroplane with motivators (control surfaces) fixed. It is not surprising, therefore, that attempts have been made to draw conclusions about trends in an aeroplane's stability on the basis of a less complete knowledge of the coefficients of the characteristic equation. Gates, through a series of papers culminating in the well-known generalized theory of stability and control analysis<sup>6</sup> (written jointly with Miss H.M. Lyon) investigated the special significance of the constant term and the coefficient of  $\lambda^2$  of the longitudinal stability quartic, their relationship to the static and manoeuvre margins and the implications of changes in sign of these margins for the stability of the longitudinal modes of motion of an aeroplane.

Algebraic criteria such as those given by Routh and Hurwitz often lead to conditions the interpretation of which is difficult. To overcome this difficulty and to extract the utmost generality from specific calculations of the roots of the stability, the alternative approach of displaying in graphical form the dependence of the stability on the values of system parameters was adopted. In the case of a single system parameter, the variation of the roots of the stability equation can be presented in the form of a one-parameter stability diagram or a root-locus diagram.

No doubt one of the factors contributing to the pursuit of simplified criteria and studies of general trends was the tedium then attending the determination of the roots of the characteristic equation. An alternative approach was to seek approximate solutions<sup>7</sup> for the roots of the characteristic equation. Nowadays, the relative ease with which the roots can be extracted using even the small, readily available, desk computers could be taken to indicate that studies of general trends and simplified criteria become less important. The validity of this argument is questionable and adoption of that viewpoint could

result in decreased insight into the nature of the basic aeroplane stability. Previously acquired knowledge could become forgotten or at best ill-remembered. Force is lent to this counter argument by the recent appearance of papers which sought to discuss the question of when static stability is a sufficient, as well as a necessary, condition for dynamic stability. The first of these by Sachs<sup>8</sup> investigated the matter using two-parameter stability boundaries and root-locus plots for specific aeroplanes. More recently Babister<sup>9</sup> suggested that the use of the approximate factorization of the longitudinal stability quartic, due to Bairstow, afforded greater insight into the matter. He was careful, however, to remark that the conclusions can only be relied upon when the degree of approximation is good.

The quartic equation can be written as,

$$K_4 \lambda^4 + K_3 \lambda^3 + K_2 \lambda^2 + K_1 \lambda + K_0 = 0$$

or

$$K_4 (\lambda^2 + g\lambda + h) (\lambda^2 + G\lambda + H) = 0 \quad ,$$

where the two factors always exist and have real coefficients. Previous experience of the relationships between the coefficients of the original quartic ( $K_4, K_3, K_2, K_1$  and  $K_0$ ) and those of the two quadratic factors ( $g, h, G$  and  $H$ ) suggested to the present author that  $g(G)$  is related to  $h(H)$  when one parameter of the system is varied all others being held constant. The present analysis derives such relationships and demonstrates that they are relatively simple in form. The existence of these relationships enables diagrams to be constructed from which conclusions may be drawn concerning the variation in the nature and stability of the individual modes as a particular system parameter changes.

Although differing from the one-parameter stability diagram and the exact form of the root-locus plot in that it does not require the roots of the quartic to be determined, the present method provides all the data necessary to construct either of the other two diagrams, but to do so requires the solution of the two quadratics.

## 2 RELATIONSHIP OF THE COEFFICIENT OF THE QUADRATIC FACTORS TO THOSE OF THE QUARTIC

In the main text the notation of R&M 3562<sup>1</sup> is adopted, but for ease of comparison with Babister's analysis<sup>9</sup> and the results of other references<sup>6,7,11</sup> the analysis is repeated in Appendix A in terms of the Neumark-type notation<sup>6</sup>.

The stability of the small perturbation longitudinal motion of an aircraft, with controls fixed, from a trimmed rectilinear flight condition in a constant density atmosphere is governed by the quartic<sup>10</sup>

$$K_4 \lambda^4 + K_3 \lambda^3 + K_2 \lambda^2 + K_1 \lambda + K_0 = 0 \quad (1)$$

$$\begin{aligned} \text{where } K_4 &= Q_{m4}, \\ K_3 &= Q_{m3} + m_q Q_{m4} + m_w W_{m3}, \\ K_2 &= Q_{m2} + m_q Q_{m3} + m_w W_{m2} + m_w W_{m3} + m_u U_{m3}, \\ K_1 &= m_q Q_{m2} + m_w W_{m1} + m_w W_{m2} + m_u U_{m2}, \\ K_0 &= m_w W_{m1} + m_u U_{m1}, \end{aligned}$$

$$\begin{aligned} \text{and } Q_{m4} &= 1 + z_{\dot{w}} \approx 1, \\ Q_{m3} &= x_u + z_w + (x_u z_{\dot{w}} - z_u x_{\dot{w}}) \approx x_u + z_w, \\ Q_{m2} &= x_u z_w - z_u x_w, \\ W_{m3} &= u_e - z_q \approx u_e, \\ W_{m2} &= u_e x_u + w_e z_u + (z_u x_q - x_u z_q) - g_2 \approx u_e x_u + w_e z_u - g_2, \\ W_{m1} &= g_1 z_u - g_2 x_u, \\ U_{m3} &= -x_q - w_e + (z_q x_{\dot{w}} - z_{\dot{w}} x_q) - u_e x_{\dot{w}} - w_e z_{\dot{w}} \approx -w_e, \\ U_{m2} &= (x_w z_q - z_w x_q) - g_1 (1 + z_{\dot{w}}) - g_2 x_{\dot{w}} - u_e x_w - w_e z_u \approx -g_1 - u_e x_w - w_e z_u, \\ U_{m1} &= -g_1 z_w + g_2 x_w. \end{aligned}$$

The characteristic equation as given applies to any body system of axes, but it is possible to simplify the expressions, without any essential loss of generality, by adopting aerodynamic body axes (so-called stability axes) and restricting our attention to a level flight equilibrium condition. In this case the following relationships apply,

$$u_e = 1, \quad w_e = 0, \quad g_1 = g \quad \text{and} \quad g_2 = 0.$$

It is convenient to conduct the analysis in terms of dynamic normalized equivalents of the physical quantities. The previous expressions for the W's and the U's reduce to

$$\begin{aligned} W_{m3} &= 1; & U_{m3} &= 0; \\ W_{m2} &= x_u; & U_{m2} &= -\dot{g} - x_w; \\ W_{m1} &= \dot{g} z_u; & U_{m1} &= -\dot{g} z_w. \end{aligned}$$

so that the coefficients of the quartic may be written as

$$K_4 = 1$$

$$K_3 = Q_{m_3} + m_q + m_w^*$$

$$K_2 = Q_{m_2} + m_q Q_{m_3} + m_w^* W_{m_2} + m_w$$

$$K_1 = m_q Q_{m_2} + m_w^* W_{m_1} + m_w W_{m_2} + m_u U_{m_2}$$

$$K_0 = m_w W_{m_1} + m_u U_{m_1} .$$

As remarked in the Introduction the quartic can always be factorized into two quadratic factors. Thus,

$$\lambda^4 + K_3 \lambda^3 + K_2 \lambda^2 + K_1 \lambda + K_0 = (\lambda^2 + g\lambda + h)(\lambda^2 + G\lambda + H) = 0 . \quad (2)$$

An advantage of the two quadratic factors lies in the simpler statement for the necessary and sufficient conditions for stability in terms of  $g, h, G$  and  $H$  rather than in terms of  $K_3, K_2, K_1$  and  $K_0$ . For the former the conditions are:

$$g > 0, \quad h > 0; \quad G > 0, \quad H > 0$$

whilst in terms of the coefficients of the original quartic the necessary and sufficient conditions for stability are

$$K_3 > 0, \quad K_1 > 0, \quad K_0 > 0 \quad \text{and} \quad R > 0$$

where  $R$  (the Routh discriminant) is  $K_3 K_2 K_1 - K_1^2 - K_3^2 K_0$ .

An essential step in the analysis in terms of  $g, h$  or  $G, H$  is the relationship between these and the coefficients  $K_3, K_2, K_1$  and  $K_0$ .

Expansion of the product of the two quadratic factor yields the following

$$\left. \begin{aligned} G + g &= K_3 \\ H + h + gG &= K_2 \\ Hg + Gh &= K_1 \\ Hh &= K_0 \end{aligned} \right\} \quad (3)$$



Since subsequently we shall regard  $m_w$  and  $m_u$  as parameters which may be varied, whilst other quantities involved in  $K_3$ ,  $K_2$ ,  $K_1$  and  $K_0$  are held constant, the coefficients are rewritten as

$$K_2 = k_2 + m_w$$

$$K_1 = k_1 + m_w W_{m_2} + m_u U_{m_2}$$

$$K_0 = m_w W_{m_1} + m_u U_{m_1} .$$

Manipulation of the above relationships between the two sets of coefficients yields the following equations,

$$\left. \begin{aligned} K_2 g - K_1 + K_3 h &= 2gh + g^2(K_3 - g) \\ K_2 h - K_0 &= gh(K_3 - g) + h^2 \end{aligned} \right\} \quad (4)$$

An identical pair of equations relate  $G$  and  $H$  by virtue of the symmetry of the basic equations.

To obtain the Bairstow approximations used by Babister<sup>9</sup> the assumption is made that  $g$  and  $h$ , which may be identified with the phugoid motion, are small so that to this degree of approximation,

$$K_2 h - K_0 = 0 \quad \text{or} \quad h = \frac{K_0}{K_2}$$

and

$$K_2 g - K_1 + K_3 h = 0 \quad \text{or} \quad g = \frac{(K_2 K_1 - K_3 K_0)}{K_2^2} .$$

Furthermore since  $g$  and  $h$  are small,

$$G = K_3 - g \approx K_3$$

and

$$H = K_2 - h - gG \approx K_2 .$$

These various approximations may be improved upon by an iterative solution. However our objective is not to obtain approximate values of  $g$  and  $h$  or the roots associated with this factor, but to examine the manner in which  $g$  and  $h$

are related when a single parameter (for example  $m_u$ ) is varied. We accordingly return to equations (4).

### 3 RELATIONSHIP OF $g(G)$ TO $h(H)$ WHEN $m_u$ IS VARIED

Introduction of the expressions for  $K_1$  and  $K_0$  into equations (4) yields the following pair of equations,

$$\left. \begin{aligned} U_{m_2} m_u &= K_2 g + K_3 h - k_1 - W_{m_2} (K_2 - k_2) - 2gh - g^2 (K_3 - g) \\ U_{m_1} m_u &= K_2 h - W_{m_1} (K_2 - k_2) - gh (K_3 - g) - h^2 \end{aligned} \right\} \quad (5)$$

These two equations imply that as  $m_u$  is varied the associated values of  $g$  and  $h$  satisfy the relationship,

$$k = \frac{U_{m_2}}{U_{m_1}} = \frac{k_1 + W_{m_2} (K_2 - k_2) - K_3 h - K_2 g + 2gh + g^2 (K_3 - g)}{W_{m_1} (K_2 - k_2) - K_2 h + gh (K_3 - g) + h^2} \quad (6)$$

This exact relationship between  $g$  and  $h$  can be rearranged as a quadratic for  $h$  in terms  $g$ , thus,

$$\alpha_2 h^2 + \alpha_1 h + \alpha_0 = 0 \quad (7)$$

where  $\alpha_2 = k$

$$\alpha_1 = -kg^2 + (K_3 k - 2)g + (K_3 - K_2 k)$$

$$\alpha_0 = g^3 - K_3 g^2 + K_2 g + (kW_{m_1} - W_{m_2})(K_2 - k_2) - k_1$$

Approximations to equation (7) may be formed.

- (1) Treat both  $g$  and  $h$  as small (appropriate when isolating the phugoid factor)

Equation (7) may be then approximated by the linear relationship

$$\alpha_1 h + \alpha_0 = 0$$

where  $\alpha_1 \rightarrow (K_3 k - 2)g + (K_3 - K_2 k)$

and  $\alpha_0 \rightarrow K_2 g + (kW_{m_1} - W_{m_2})(K_2 - k_2) - k_1$

This is the same result as obtained by Babister<sup>9</sup> by use of the Bairstow approximation to the roots of the quartic.

(2) Retain terms up to and including the product and the squares of  $g$  and  $h$

The equation has the same form as (7) with  $\alpha_0$  coefficient simplified by the omission of the term  $g^3$ , an often insignificant change.

To each pair of values of  $g$  and  $h$  that satisfy equation (7) there corresponds some value of the parameter  $m_u$  and this is given by either of the two relationships of equation (5).

As previously remarked a corresponding set of equations exists between the other two coefficients  $G$  and  $H$ . In a complete analysis it is useful, as we shall see later, to plot the curve of  $H$  as a function of  $G$  as well as of  $h$  as a function of  $g$ , because in such a case extreme values of the design parameter need to be embraced. Where, on the contrary, interest centres around the effect of modest variations from a given datum value it is more reasonable to obtain either approximate or exact values of  $g$  and  $h$  for the basic aircraft.

To illustrate the interpretation of the plot of  $h$  against  $g$  this has been displayed schematically in Fig 1. As previously noted stability is ensured if  $g > 0$  and  $h > 0$ . This positive quadrant is subdivided by the curve  $g^2 = 4h$  into regions in which the factor corresponds to a convergent oscillation and two subsidences respectively. The axes and the curve  $g^2 = 4h$  subdivide the unstable regime into different forms of instability as indicated on the diagram.

3.1 Value of  $g$  when  $h = 0$

Of special interest is the value of  $g$  when  $h$  is zero. The determination of this value of  $g$  requires the solution of a cubic equation  $\alpha_0 = 0$ , that is

$$g^3 - K_3 g^2 + K_2 g - k_1 + (K_3 - k_2)(kW_{m1} - W_{m2}) = 0.$$

The different roots corresponds to the 'phugoid' factor, which we shall generally identify with  $g$  and  $h$ , and to the 'short period' (or fast) factor ( $G$  and  $H$ ). In the case of 'phugoid' factor we may drop the term in  $g^3$  and  $g^2$  for the numerically smallest root. It is, therefore, of interest to examine more closely the constant term in the cubic for  $g$ , which we shall denote by  $K$ . Now

$$\begin{aligned}
K &= (K_3 - k_2)(kW_{m1} - W_{m2}) - k_1 \\
&= m_w \left\{ (\hat{g} + x_w) \frac{z_u}{z_w} - x_u \right\} - m_q (x_u z_w - x_w z_u) - \hat{g} z_u m_w .
\end{aligned}$$

If, for simplicity, we neglect the effects of compressibility and elastic distortion the dynamic normalized quantities involved in the above expression can be rewritten in the following forms,

$$\hat{g} = C_{Le}$$

$$x_u = -\ddot{x}_u = 2(C_D + C_{AS})_e ,$$

where  $C_{AS} = -\frac{1}{S} \frac{\partial T_{av}}{\partial Q}$ , so that  $C_{AS} = 0$  for jet propelled aircraft,

$$z_u = -\ddot{z}_u = 2C_{Le}$$

$$x_w = -\ddot{x}_w = \left( \frac{\partial C_D}{\partial \alpha} - C_L \right)_e$$

$$z_w = -\ddot{z}_w = \left( \frac{\partial C_L}{\partial \alpha} + C_D \right)_e \approx \left( \frac{\partial C_L}{\partial \alpha} \right)_e , \text{ and so}$$

$$\hat{g} + x_w = \left( \frac{\partial C_D}{\partial \alpha} \right)_e = \left( \frac{\partial C_L}{\partial \alpha} \right)_e \left( \frac{\partial C_D}{\partial C_L} \right)_e .$$

The first term in  $K$  is thus approximately,

$$- 2m_w \left( C_D + C_{AS} - C_L \frac{\partial C_D}{\partial C_L} \right)_e$$

which demonstrates the importance of whether the equilibrium speed is above or below the minimum drag speed (cf Refs 7, 9, 11) in determining the sign of  $g$  when  $h = 0$ .

If the basic value of  $g$  is positive there are three cases according as,

$$(i) \quad (g)_{h=0} > (g)_{basic} > 0 ;$$

$$(ii) \quad (g)_{basic} > (g)_{h=0} > 0 ;$$

$$(iii) \quad (g)_{\text{basic}} > 0 > (g)_{h=0} ,$$

as illustrated in Fig 1. Case (iii) arises when  $K$  is positive, that is, when  $(C_D + C_{AS} - C_L(\partial C_D / \partial C_L))$  has a sufficiently large negative value. When this is so there is a range of positive static margins for which undamped phugoid oscillations can occur (cf Appendix A and examples). An examination of the remaining terms in  $K$  indicates that small values of  $m_q$  and  $m_w^*$  make for more positive values of  $K$  and the same consequences, which is in agreement with the conclusions drawn by Babister<sup>9</sup>.

#### 4 THE $g, h$ RELATIONSHIP FOR VARYING $m_w$

Another important and basic parameter in the longitudinal stability quartic is  $m_w$ . The relationship of  $g$  to  $h$  (or  $G$  to  $H$ ) as  $m_w$  is varied can readily be found by introduction of the expressions for  $K_2, K_1$  and  $K_0$  into equations (4) and rearranging the equations obtained in the form,

$$\left. \begin{aligned} m_w(g - W_{m2}) &= k_1 + U_{m2}m_u - k_2g - K_3h + 2gh + g^2(K_3 - g) \\ m_w(h - W_{m1}) &= U_{m1}m_u - k_2h + gh(K_3 - g) + h^2 \end{aligned} \right\} \quad (8)$$

Elimination of  $m_w$  yields the desired relationship, that is

$$\frac{g - W_{m2}}{h - W_{m1}} = \frac{k_1 + U_{m2}m_u - k_2g - K_3h + 2gh + g^2(K_3 - g)}{U_{m1}m_u - k_2h + gh(K_3 - g) + h^2} \quad (9)$$

Equation (9) is the most general form of the relationship. It is instructive to introduce into the above equation the simplified forms of  $U_{m1}, U_{m2}, W_{m1}$  and  $W_{m2}$  which pertain to a level flight condition of equilibrium. We then obtain the equation,

$$\frac{g - x_u}{h - z_u C_{Le}} = \frac{k_1 - m_u(C_{Le} + x_w) - k_2g - K_3h + 2gh + g^2(K_3 - g)}{h^2 + gh(K_3 - g) - k_2h - z_w m_u C_{Le}} \quad (10)$$

This may be rewritten as a quadratic in  $h$ ,

$$\beta_2 h^2 + \beta_1 h + \beta_0 = 0 \quad (11)$$

where  $\beta_2 = K_3 - x_u - g$ ,

$$\beta_1 = \{k_2 x_u - k_1 + m_u(C_{Le} + x_w) - z_u C_{Le} K_3\} + (2z_u C_{Le} - x_u K_3)g + x_u g^2,$$

$$\beta_0 = C_{Le} \left[ \{k_1 z_u + x_u z_u m_u - z_u m_u (C_{Le} + x_w)\} - (k_2 z_u + z_w m_u)g + z_u g^2 (K_3 - g) \right].$$

From this equation the values of  $h$  may be obtained as  $g$  is varied away from its basic value as shown schematically in Fig 2. The interpretation of the different regions into which the axes and the curve  $g^2 = 4h$  divide the plane follows the pattern of Fig 1.

Various approximations to the relationship of  $h$  to  $g$  may be obtained. The simplest of these corresponds to the retention of only linear terms on the right-hand side of equations (8) or in the numerator and denominator of the right-hand side of equation (10). To this approximation (approximation I)

$$\beta_2 \approx K_3,$$

$$\beta_1 \approx k_2 x_u + m_u (C_{Le} + x_w) - k_1 - z_u C_{Le} K_3,$$

$$\beta_0 \approx C_{Le} \left[ \{k_1 z_u + x_u z_u m_u - m_u z_u (C_{Le} + x_w)\} - (z_w m_u + k_2 z_u)g \right].$$

Another form of approximation is obtained if in the expanded equation (11) terms in  $gh^2$ ,  $g^2h$  and  $g^3$  are neglected. With this adjustment (approximation II)

$$\beta_2 \approx K_3 - x_u,$$

$$\beta_1 \approx \{k_2 x_u - k_1 + m_u (C_{Le} + x_w) - z_u C_{Le} K_3\} + (2z_u C_{Le} - x_u K_3)g,$$

$$\beta_0 \approx C_{Le} \left[ \{k_1 z_u + x_u z_u m_u - z_u m_u (C_{Le} + x_w)\} - (k_2 z_u + z_w m_u)g + z_u K_3 g^2 \right].$$

With this degree of approximation the curve becomes a conic and in Appendix B the nature of conic approximations to the  $h$ ,  $g$  curves for both varying  $m_u$  and varying  $m_w$  are discussed.

It is implicit in the above approximations (and those of section 4.1) that  $g$  and  $h$  are generally small and, in the case of the longitudinal quartic, associated with the slow or 'phugoid' motion.

#### 4.1 Value of $g$ for which $h = 0$

The exact relationship between  $h$  and  $g$  reduces to the following cubic in  $g$  when  $h$  is set to zero,

$$z_u g^3 - z_u K_3 g^2 + (k_2 z_u + z_w m_u) g - \{k_1 z_u + x_u z_w m_u - z_u m_u (C_{Le} + x_w)\} = 0.$$

As a first approximation to the solution of this cubic we have,

$$\begin{aligned} g &= \frac{k_1 z_u + m_u \{x_u z_w - z_u (C_{Le} + x_w)\}}{k_2 z_u + z_w m_u} \\ &= \frac{k_1 C_{Le} + m_u \{(C_D + C_{AS})(C_{L\alpha} + C_D) - C_L C_{L\alpha} (\partial C_D / \partial C_L)\}_e}{k_2 C_{Le} + m_u C_{L\alpha}} \end{aligned}$$

where  $C_{L\alpha} = (\partial C_L / \partial \alpha)_e$ .

The term in  $m_u$  in the numerator is approximately equal to

$$m_u C_{L\alpha} \left( C_D + C_{AS} - C_L \frac{\partial C_D}{\partial C_L} \right)_e.$$

Thus we see that once more the location of the flight conditions relative to the minimum drag conditions plays an important part in determining the trends in  $g$ .

#### 5 NUMERICAL EXAMPLE

To illustrate the use of the preceding analysis we consider a basic aircraft having the following characteristics and equilibrium conditions,

$$\begin{aligned} u_1 &= 272 \\ i_y &= 1.75 \\ C_{Le} &= 0.25 \\ x_u &= 0.0188 \\ z_u &= 0.25 \end{aligned}$$

$$\begin{aligned}
 x_w &= -0.139 \\
 z_w &= 4.899 \\
 m_w &= 113.774 \\
 m_w^* &= 1.20 \\
 m_q &= 6.542 ,
 \end{aligned}$$

and with  $z_w^*$ ;  $z_q$  and  $m_u$  all zero.

To examine the effect of varying  $m_u$  on the coefficients  $g$  and  $h$ , equation (7) is solved for the values of  $g$  indicated in Fig 3. In this example the basic aircraft possesses a stable phugoid mode (convergent oscillation). As  $m_u$  is increased a region of two subsidences (very narrow) is quickly traversed and a region in which the quadratic factor corresponds to two real roots, one subsidence and one divergence, is entered. Reduction of  $m_u$  is associated with a phugoid or oscillatory motion at first convergent but eventually becoming divergent.

By use of equation (11) the effect of varying  $m_w$  may be determined. The values of  $h$  for the values of  $g$  indicated in Fig 4 yield, for the example aircraft, the curve shown in that figure. As the value of  $m_w$  is increased this curve is traversed in the direction indicated. Most of the curve remains within the convergent oscillation region and it just enters the one subsidence, one divergence region near  $g = 0.03$ .

#### 6 VALUES OF THE PARAMETERS $m_u$ AND $m_w$ ASSOCIATED WITH POINTS OF THE $h, g$ CURVE

To each point of the  $h, g$  curve there corresponds a value of the design parameter being varied, namely,  $m_u$  or  $m_w$ , as the case may be.

The values are given by either of the two equations (5) for  $m_u$ , when this is the parameter being varied and by either of the two equations (8) for  $m_w$  when this is being varied. When either (or both) of the factors  $(\lambda^2 + g\lambda + h)$  and  $(\lambda^2 + G\lambda + H)$  represents an oscillation no difficulty arises in the computation of the parameter values. However, when these two quadratic factors themselves factorize into two pairs of real roots the matter is not straightforward. Suppose the factors are  $(\lambda + R_1)$ ,  $(\lambda + R_2)$ ,  $(\lambda + r_1)$ ,  $(\lambda + r_2)$  then all six combinations of these in pairs must occur somewhere along the  $g, h$  curve or the  $G, H$  curve, since the analysis cannot make the distinction. It is for this reason that the simultaneous plotting of the  $g, h$  and the  $G, H$



curve is desirable. The matter is discussed in more detail in relation to the numerical examples given in Appendix A.

7 ANALYSIS IN TERMS OF THE PARAMETERS  $K_n$ , STATIC MARGIN AND  $H_m$ , MANOEUVRE MARGIN

The well-known criteria for stability of the longitudinal motion of an aircraft (static and manoeuvre margins) are related to  $m_u$  and  $m_w$  as follows,

$$K_n = \frac{i_y}{\mu_1} \frac{1}{C_{Le}(C_{L\alpha})_e} \left\{ \left( C_L + \frac{v}{2} \frac{\partial C_L}{\partial v} \right)_e m_w - \frac{1}{2} (C_{L\alpha} + C_D)_e m_u \right\}$$

and

$$H_m = \frac{i_y}{\mu_1 (C_{L\alpha})_e} (m_w + C_{L\alpha} m_q)_e \quad (\text{cf Appendix A}).$$

Thus the coefficients of the quartic may be expressed in terms of  $K_n$  and  $H_m$  in place of  $m_u$  and  $m_w$ . The coefficients affected are  $K_2$ ,  $K_1$  and  $K_0$ . These may be written in the form,

$$K_2 = K_{2m} H_m + K_{20}$$

$$K_1 = K_{1m} H_m + K_{1n} K_n + K_{10}$$

and

$$K_0 = K_{0n} K_n$$

where  $K_{20} = k_2 - m_q z_w$ ,

$$K_{10} = k_1 - m_q \{ x_u z_w - z_u (C_{Le} + x_w) \},$$

$$K_{2m} = \mu_1 z_w / i_y,$$

$$K_{1m} = (\mu_1 / i_y) \{ x_u z_w - z_u (C_{Le} + x_w) \},$$

$$K_{1n} = (2\mu_1 / i_y) C_{Le} (C_{Le} + x_w),$$

$$K_{0n} = (2\mu_1 / i_y) C_{Le}^2 z_w,$$

when the approximation

$$z_w = \frac{\partial C_L}{\partial \alpha} + C_D \approx \frac{\partial C_L}{\partial \alpha}$$

is made.

By introduction of the relationships appropriate to level flight, viz,

$$x_u = 2 \left( c_D + \frac{v}{2} \frac{\partial c_D}{\partial v} \right)_e ,$$

$$z_u = 2 \left( c_L + \frac{v}{2} \frac{\partial c_L}{\partial v} \right)_e ,$$

$$x_w = \left( \frac{\partial c_D}{\partial \alpha} - c_L \right)_e ,$$

$$z_w = \left( \frac{\partial c_L}{\partial \alpha} + c_D \right)_e \approx \frac{\partial c_L}{\partial \alpha} ,$$

the above can be expressed in terms of  $c_D$ ,  $c_L$  and their derivatives.

With the coefficients of the quartic expressed in terms of  $K_n$  and  $H_m$  we can establish the locus of the points  $g$ ,  $h$  and  $G$ ,  $H$  as each parameter is varied in turn, all other parameters being held constant. From equations (4) we have,

$$\left. \begin{aligned} (K_{2m}g - K_{1m})H_m - K_{1n}K_n &= K_{10} - K_{20}g - K_3h + 2gh + g^2(K_3 - g) \\ K_{2m}hH_m - K_{0n}K_n &= h^2 + gh(K_3 - g) - K_{20}h \end{aligned} \right\} \quad (12)$$

Elimination of  $K_n$  gives the locus for varying  $K_n$  and this is

$$\frac{K_{1n}}{K_{0n}} = \frac{(K_{10} + K_{1m}H_m) - (K_{20} + K_{2m})H_m - K_3h + 2gh + g^2(K_3 - g)}{h^2 + gh(K_3 - g) - h(K_{20} + K_{2m}H_m)} . \quad (13)$$

Elimination of  $H_m$  yields the relationship satisfied for varying  $H_m$ , that is

$$\frac{K_{2m}g - K_{1m}}{K_{2m}h} = \frac{(K_{10} + K_{1n}K_n) + K_{20}g - K_3h + 2gh + g^2(K_3 - g)}{h^2 + gh(K_3 - g) - hK_{20} + K_{0n}K_n} . \quad (14)$$

By virtue of the linear relationship between  $H_m$  and  $m_w$ , a fixed value of one implies a fixed value of the other. Consequently, the curves for varying  $K_n$  (equation (13)) is identical to equation (6). However a fixed value of the static margin,  $K_n$ , implies a linear relationship of  $m_u$  and  $m_w$  as  $H_m$  is

varied. In this case  $K_0$  maintains a constant value proportional to  $K_n$ . This is illustrated by the results shown in Figs 18 and 19, although it should be noted that these results are in terms of the old notation (see List of symbols and Appendix A).

## 8 DISCUSSION

The analysis of a number of different cases enables some comments to be made as regards the stability of the different longitudinal modes of motion and their dependence on design features. These are in agreement with those of Refs 6, 7, 8, 9 and 11.

From the equation of the  $g, h$  locus for varying  $\kappa$  and varying  $\omega$  respectively it is possible to deduce the value of  $g$  when  $h = 0$  and to demonstrate its strong dependence on the relation of the equilibrium speed to the minimum drag speed. This is illustrated by Figs 5 and 6.

Cases can exist for which increase in the static margin ( $K_n$  or decrease in  $\kappa$ ) results in an unstable phugoid oscillation, for example, aircraft 3 of Fig 5. It is worth noting that the factor  $(\lambda^2 + G\lambda + H)$  represents the usual short-period oscillation of aircraft 1, 2 and 3 and that the values of  $G$  and  $H$  only change slightly for the range of  $g$  covered in Fig 5. Each of the aircraft 1, 1a and 3 of Figs 5 and 6 is statically stable ( $E > 0$ ) for points within the unstable oscillation region (see also section 4 of Appendix A).

Variation of  $\omega$  with all other parameters held constant shows that aircraft 1 and 2 (Fig 7) possess unstable phugoids for a certain range of  $\omega$  in spite of being statically stable (see section 5 of Appendix A).

The cases illustrated in Figs 8 and 9 point to the danger of a positive static margin in conjunction with a negative or zero manoeuvre margin, which can give rise to a rapid divergence or a markedly unstable phugoid oscillation. It should be noted that for the cases illustrated in Figs 8 and 9 when both  $g$  and  $h$  are positive,  $H$  must be negative for a negative static margin ( $K_n$ ) (or a negative  $E$ ). This implies a divergence in pitch. In contrast, with the values of manoeuvre margin indicated in Fig 10, a divergence is associated with the negative static margin. As pointed out in Ref 6 this divergence may be sufficiently slow to be tolerated if the manoeuvre margin is sufficiently large and positive as suggested by the trend with increasing manoeuvre margin.

With a fixed value of  $\kappa = -0.085$ , variation of  $\omega$ , for the aircraft which is the subject of Figs 13 and 14, demonstrates stability of all modes for

$\omega > -2.663$  . (This corresponds to  $K_n = 0$ ,  $H_m = 0.01$  .) Analysis in terms of manoeuvre margin for the same aircraft, but with the static margin held at 0.05, again demonstrates the link between unstable phugoid oscillation and a small manoeuvre margin with this level of static stability.

## 9 CONCLUSIONS

- (1) It is possible to relate the coefficients of the two quadratic factors, into which it is always possible to factorize a quartic stability equation, to those of the quartic.
- (2) The relatively simple nature of the relationships between the coefficients provides a method of analysing the stability of the longitudinal motion of an aircraft as a single design parameter is varied.
- (3) A stability analysis of this form is intermediate between the one-parameter diagram and a root-locus plot. It does not, however, involve solution of a number of quartics. It also possesses a compactness certainly not present in the one-parameter diagram.
- (4) Use of the present method enables certain broad trends to be established, see section 8.
- (5) Here the application of the method has been to the longitudinal stability quartic. It is equally applicable to analysis of the lateral stability quartic and extension to higher-order stability equations may be possible.

## Appendix A

### ANALYSIS OF THE QUARTIC IN TERMS OF THE NOTATION OF R&M 2027

#### A.1 Analysis for the design parameters $\omega$ and $\kappa$

Babister<sup>9</sup> uses the notation of R&M 2027 and to facilitate comparison with his analysis and the results of a number of past papers it is useful to analyse the quartic using this old notation.

The stability quartic for small perturbation longitudinal motion about steady level flight in a uniform atmosphere has the same form, but the numerical value of the coefficients and roots differ from those of the dynamic normalized equation of the main text. We write it in the form,

$$\lambda^4 + B\lambda^3 + C\lambda^2 + D\lambda + E = 0 \quad (A-1)$$

where (see Refs 6, 7, 9 or 11)

$$\begin{aligned} B &= N + v + \chi, \\ C &= \omega + Nv + Q\chi + P, \\ D &= Q\omega - S\kappa + Pv + R\chi, \\ E &= R\omega - T\kappa. \end{aligned}$$

Corresponding to equations (4) of the main text, section 2, we have,

$$\left. \begin{aligned} Cg - D + Bh &= 2gh + g^2(B - g) \\ Ch - E &= gh(B - g) + h^2 \end{aligned} \right\} \quad (A-2)$$

If the above expressions for C, D and E are inserted in these equations they can be written as

$$\left. \begin{aligned} (g - Q)\omega + S\kappa &= Pv + R\chi - (P + Nv + Q\chi)g - Bh + 2gh + g^2(B - g) \\ (h - R)\omega + T\kappa &= -(P + Nv + Q\chi)h + gh(B - g) + h^2 \end{aligned} \right\} \quad (A-3)$$

Thus, if we require the relationships of h and g as  $\kappa$  is varied all other parameters being held constant it is necessary to eliminate  $\kappa$ . This yields

$$\frac{S}{T} = \frac{(Pv + R\chi + Q\omega) - (\omega + P + Nv + Q\chi)g - Bh + 2gh + g^2(B - g)}{R\omega - (\omega + P + Nv + Q\chi)h + gh(B - g) + h^2} \quad (A-4)$$

For varying  $\omega$  the relationship is given by

$$\frac{g - Q}{h - R} = \frac{(Pv + R\chi - S\kappa) - (P + Nv + Q\chi)g - Bh + 2gh + g^2(B - g)}{-T\kappa - (P + Nv + Q\chi)h + gh(B - g) + h^2} \quad (A-5)$$

As remarked in the main text the value of  $\kappa$  corresponding to a given point of the curve defined by equation (A-4) is given by either of the two equations,

$$S\kappa = (Pv + R\chi + Q\omega) - (\omega + P + Nv + Q\chi)g - Bh + 2gh + g^2(B - g) \quad (A-6)$$

or

$$T\kappa = R\omega - (\omega + P + Nv + Q\chi)h + gh(B - g) + h^2 \quad (A-7)$$

Likewise for a point on the curve defined by equation (A-5) the value of  $\omega$  is given by either

$$(g - Q)\omega = (Pv + R\chi - S\kappa) - (P + Nv + Q\chi)g - Bh + 2gh + g^2(B - g) \quad (A-8)$$

or

$$(h - R)\omega = -T\kappa - (P + Nv + Q\chi)h + gh(B - g) + h^2 \quad (A-9)$$

It may be noted that as

$$h \rightarrow R, \quad \omega \rightarrow \pm \infty$$

also as

$$G \rightarrow Q, \quad \omega \rightarrow \pm \infty.$$

Since equations (A-8) and (A-9) yield identical values of  $\omega$  (this generally provides an arithmetical check) the point (Q,R) is a point of the curve, which approached from one side corresponds to  $\omega \rightarrow +\infty$  and from the other side to  $\omega \rightarrow -\infty$ . Since Q and R are usually positive this point lies in the first quadrant.

A discussion of the geometry of the curves defined by equations (A-4) and (A-5) is given in Appendix B.

## A.2 Analysis in terms of $H_m$ and $K_n$

Instead of expressing the coefficients C, D and E in terms of  $\omega$  and  $\kappa$  we may express them in terms of the stability margins  $H_m$  and  $K_n$  and then examine the effect of varying either of these two parameters on the stability characteristics.

The static and manoeuvre margins,  $K_n$  and  $H_m$ , as usually defined are

$$K_n = \frac{i_B}{\mu} \frac{2\ell}{\bar{c}} \frac{1}{C_L C_{L\alpha}} \left\{ \left( C_L + \frac{V}{2} \frac{\partial C_L}{\partial V} \right) \omega - \frac{1}{2} C_{L\alpha} \kappa \right\} \quad (A-10)$$

and

$$H_m = \frac{i_B}{\mu} \frac{2\ell}{\bar{c}} \frac{1}{C_{L\alpha}} (\omega + \frac{1}{2} C_{L\alpha} v) \quad (A-11)$$

Here level flight equilibrium conditions have been assumed and the approximation  $\frac{1}{2}(C_{L\alpha} + C_D) \approx \frac{1}{2}C_{L\alpha}$  made. From these relationships we have,

$$\omega = \frac{\mu}{i_B} \left( \frac{\bar{c}}{2\ell} \right) C_{L\alpha} H_m - \frac{1}{2} C_{L\alpha} v$$

and

$$\kappa = \frac{\mu}{i_B} \left( \frac{\bar{c}}{\ell} \right) \left( C_L + \frac{V}{2} \frac{\partial C_L}{\partial V} \right) H_m - \frac{\mu}{i_B} \left( \frac{\bar{c}}{\ell} \right) C_L K_n - \left( C_L + \frac{V}{2} \frac{\partial C_L}{\partial V} \right) v$$

so that

$$C = C_m H_m + (N - \frac{1}{2} C_{L\alpha}) v + Q\chi + P,$$

$$D = D_m H_m + D_n K_n + \left\{ P + \left( C_L + \frac{V}{2} \frac{\partial C_L}{\partial V} \right) S \right\} v + R\chi,$$

$$E = E_n K_n$$

where  $C_m = \frac{\mu}{i_B} \left( \frac{\bar{c}}{2\ell} \right) C_{L\alpha},$

$$D_m = \frac{\mu}{i_B} \left( \frac{\bar{c}}{\ell} \right) \left\{ \frac{1}{2} C_{L\alpha} Q - \left( C_L + \frac{V}{2} \frac{\partial C_L}{\partial V} \right) S \right\},$$

$$D_n = \frac{\mu}{i_B} \left( \frac{\bar{c}}{\ell} \right) C_L S,$$

and

$$E_n = \frac{\mu}{i_B} \left( \frac{\bar{c}}{2\ell} \right) C_L C_{L\alpha}.$$

If the expressions for  $C$ ,  $D$  and  $E$  are introduced into equations (A-2), we have in place of (A-3) the following,

$$\begin{aligned}
 (C_m g - D_m) H_m - D_n K_n &= \left\{ P + (C_L + \frac{1}{2} V (\partial C_L / \partial V)) S \right\} v + R_X - \left\{ P + Q_X + (N - \frac{1}{2} C_{L_\alpha}) v \right\} g \\
 &\quad - Bh + 2gh + g^2 (B - g) \\
 \text{and} \\
 h C_m H_m - E_n K_n &= - \left\{ P + Q_X + (N - \frac{1}{2} C_{L_\alpha}) v \right\} h + gh(B - g) + h^2,
 \end{aligned}
 \tag{A-12}$$

which yield for the relationship between  $h$  and  $g$  for varying  $K_n$  only the equation,

$$\frac{D_n}{E_n} = \frac{[D_m H_m + R_X + \{P + (C_L + \frac{1}{2} V (\partial C_L / \partial V)) S\} v] - \{C_m H_m + P + Q_X + (N - \frac{1}{2} C_{L_\alpha}) v\} g - Bh + 2gh + g^2 (B - g)}{h^2 + gh(B - g) - \{C_m H_m + P + Q_X + (N - \frac{1}{2} C_{L_\alpha}) v\} h}
 \tag{A-13}$$

whilst if  $K_n$  is held constant along with the other parameters and  $H_m$  varied  $h$  and  $g$  are related according to the equation,

$$\frac{(C_m g - D_m)}{C_m h} = \frac{\{D_n K_n + (P + C_L + \frac{1}{2} V (\partial C_L / \partial V)) v + R_X\} - \{P + Q_X + (N - \frac{1}{2} C_{L_\alpha}) v\} g - Bh + 2gh + g^2 (B - g)}{E_n K_n - \{P + Q_X + (N - \frac{1}{2} C_{L_\alpha}) v\} h + gh(B - g) + h^2}
 \tag{A-14}$$

From the equations for  $\omega$  and  $\kappa$  in terms of  $H_m$  and  $K_n$  it can be deduced that equation (A-13) defines the same curve as equation (A-4). In contrast varying  $H_m$  (with  $K_n$  held constant) may not be identified with varying  $\omega$ , since it also implies a varying value of  $\kappa$ . This reflects the natural character of  $\omega$  and  $\kappa$  (or  $K_n$ ) as parameters of the aircraft or, in other words, the fact that  $K_n$  is based on an exact theory whilst  $H_m$  is the result of an approximate theory. The point  $g, h$  corresponds to some value of  $K_n$  and  $H_m$  and these latter may be deduced from either of the two equations formed from equations (A-12) (cf equations (A-6) to (A-9)). The value of  $H_m \rightarrow \pm\infty$  as the point  $h = 0, g = D_m/C_m$  is approached.



### A.3 Numerical examples

Some of the features of the analysis are best illustrated by numerical examples. Again to aid in comparison of the results and conclusions with those of earlier investigations the numerical work is in terms of the old notation and the basic data drawn from Refs 6, 7 and 11.

The characteristics of the four basic aircraft considered initially are listed below.

#### Aircraft 1:

$$\begin{aligned} C_L &= 0.8, & \omega &= 25.00, & \kappa &= 0, \\ v &= 1, \quad \chi &= 0.4, & C_{L\alpha} &= \frac{\partial C_L}{\partial \alpha} = 4.0, & C_{AS} &= 0.01, \\ C_{D0} &= 0.01, & s &= 0.0625, & C_D &= C_{D0} + sC_L^2 = 0.05. \end{aligned}$$

#### Aircraft 2:

$$\begin{aligned} C_L &= 0.2, & \omega &= 25.00, & \kappa &= -21.00, \\ v &= 1, \quad \chi &= 0.4, & C_{L\alpha} &= 4.0, & C_{AS} &= 0.01, \\ C_{D0} &= 0.01, & s &= 0.0625, & C_D &= C_{D0} + sC_L^2 = 0.0125. \end{aligned}$$

#### Aircraft 3:

$$\begin{aligned} C_L &= 0.8, & \omega &= 8.0, & \kappa &= 0.4923, \\ v &= 1, \quad \chi &= 0.4, & C_{L\alpha} &= 4.0, & C_{AS} &= 0.01, \\ C_{D0} &= 0.01, & s &= 0.0625, & C_D &= C_{D0} + sC_L^2 = 0.05. \end{aligned}$$

#### Aircraft 1a:

As for aircraft 1 but with  $s$  increased to 0.08, which gives  $C_D = 0.0612$ .

The loci of the coefficients  $g, h$  are traced for these aircraft when (a)  $\kappa$  is assumed to vary, and (b) when  $\omega$  is assumed to vary, all other parameters being held constant in each case.

Spitfire V (aircraft of R&M 2027):

This aircraft was used in the numerical examples of Ref 4 and so we can quote the coefficients of the stability quartic as functions of  $\omega$  and  $\kappa$  given therein,

$$\begin{aligned} B &= 6.010 \\ C &= 5.738 + \omega \\ D &= 0.1189 + 0.03039\omega - 0.01763\kappa \\ E &= 0.002357\omega - 0.07365\kappa . \end{aligned}$$

Static and manoeuvre margins:

$$\begin{aligned} K_n &= 0.003597\omega - 0.1124\kappa \\ H_m &= 0.01914 + 0.003432\omega . \end{aligned}$$

The coefficient of  $\omega$  in  $K_n$  has been adjusted slightly as compared with the value given in R&M 2027 in order to render  $K_n \propto E$  (as it should be).

The variation of  $\kappa$  with fixed values of  $\omega$  and variation of  $\omega$  with fixed values of  $\kappa$  are considered. An analysis in terms of  $K_n$  and  $H_m$  is also considered.

Aircraft of R&M 2078 <sup>7</sup>:

In Ref 7, Neumark analysed the stability of an aircraft at two lift coefficients in terms of its dependence on the parameter  $\omega$  by means of a one-parameter stability diagram. The same data are used as a further example of the use of (g,h) and (G,H) plots.

In this case,

$$\begin{aligned} C_L &= 1.0 , \quad C_{D0} = 0.02 , \quad C_{AS} = 0.01 , \quad s = 0.06 , \\ \frac{\partial C_L}{\partial \alpha} &= 4.5 , \quad v = 3 , \quad \chi = 1 , \quad \kappa = 0 . \end{aligned}$$

A.4 Effect of varying  $\kappa$  on the stability of aircraft 1, 2 and 3

The characteristics of the three aircraft designated aircraft 1, 2 and 3 in Fig 5 were chosen such that the locus of g, h for varying  $\kappa$  corresponds to a different one of the three cases illustrated diagrammatically in Fig 1.

Datum values of h, g were obtained by solution of the stability quartic (square symbols) and also by use of the relationship of equation (A-4) (circle symbols). For all three cases the locus of g, h is close to the straight line

approximation obtained by treating both  $g$  and  $h$  as small (see section 3). In the case of aircraft 3 some departure from near linearity is evident as  $\kappa$  is decreased and the region of unstable oscillation is entered.

In the case of aircraft 1 increase of  $\kappa$  takes the aircraft out of the stable region and just into the region of unstable oscillation before entering the region where the factor  $(\lambda^2 + g\lambda + h)$  corresponds to one subsidence and one divergence. If the value of  $\partial C_D / \partial C_L$  is increased (aircraft 1a) this trend is more pronounced as shown in Fig 6. At  $g = 0$ ,

$$\kappa = \frac{h^2 - Ch + R\omega}{T} \quad (A-15)$$

and by the second of equations (A-2)

$$E = R\omega - T\kappa = Ch - h^2.$$

Thus  $E > 0$  and each of the aircraft 1, 1a and 3 is statically stable even when  $\kappa$  is such that it enters the unstable region.

The linear approximation to the locus of  $g, h$  for varying  $\kappa$  is obtained by ignoring all terms on the right-hand side of equations (A-2), that is, equation (A-4) reduces to,

$$\begin{aligned} \frac{S}{T} &= \frac{(Pv + R\chi + Q\omega) - (\omega + P + Nv + Q\chi)g}{R\omega - (\omega + P + Nv + Q\chi)h} \\ &= \frac{(Pv + R\chi + Q\omega) - Cg}{R\omega - Ch}. \end{aligned} \quad (A-16)$$

#### A.5 Locus of $g, h$ for varying $\omega$ , all other parameters constant for aircraft 1, 2 and 3

We now examine the effect on the values of  $g$  and  $h$  of varying the parameter  $\omega$  for aircraft 1, 2 and 3. For the variation of  $\omega$  in the neighbourhood of the basic aircraft the resulting curves correspond to three of the various possibilities illustrated in Fig 2. At  $g = 0$ ,

$$\omega = \frac{Bh - (Pv + R\chi - S\kappa)}{Q} \quad \text{or} \quad \frac{h^2 - (P + Nv + Q\chi)h - T\kappa}{(h - R)} \quad (A-17)$$

and

$$E = Ch - h^2 = (\omega + P + Nv + Q_X)h - h^2$$

$$= \frac{h[R\{h - (P + Nv + Q_X)\} - T_K]}{h - R} . \quad (A-18)$$

The curves for aircraft 1 and aircraft 2 (see Fig 7) intercept the positive  $h$  axis at  $h = 0.15265$  and  $0.25064$ , and at  $0.38798$ . When the values of  $\omega$  and  $E$  are determined for these points it is found that for  $7.73 > \omega > 2.04$  aircraft 1 enters the unstable oscillation region even though  $E$  (or static margin) is positive. Aircraft 2 enters the same region at  $\omega < 9.65$ . Aircraft 3 does not exhibit instability for the range of values covered by Fig 7, which corresponds to values of  $\omega$  from 2.23 up to  $+\infty$ . For some negative value of  $\omega$  it is possible that the locus of  $g, h$  intercepts the boundary  $g^2 = 4h$ , cf Fig 1 or 8.

The exact relationship of  $h$  and  $g$  for varying  $\omega$  (equation (A-5)) can be written as a quadratic in  $h$  (this is the form convenient for computation). If we write the quadratic as,

$$B_2 h^2 + B_1 h + B_0 = 0 \quad (A-19)$$

then

$$B_2 = B - Q - g ,$$

$$B_1 = \{Q(P + Nv + Q_X) - (Pv + R_X - S_K) + BR\} - (BQ - 2R)g + Qg^2 ,$$

$$B_0 = \{R(Pv + R_X - S_K) + T_K\} - \{R(P + Nv + Q_X) + T_K\}g + Rg^2(B - g) .$$

As with the corresponding equation of the main text (equation 11) it is possible to approximate to this.

#### Approximation 1:

Linearize the expressions on the right-hand side of equations (A-3) and the following results,

$$\frac{g - Q}{h - R} = \frac{(Pv + R_X - S_K) - Bh - (P + Nv + Q_X)g}{-T_K - (P + Nv + Q_X)h} . \quad (A-20)$$

which yields the following expressions for  $B_2$ ,  $B_1$  and  $B_0$ ,

$$B_2 = B ,$$

$$B_1 = Q(P + Nv + QX) - (Pv + R_X - S_K) + BR ,$$

$$B_0 = \{R(Pv + R_X - S_K) + T_K\} - \{R(P + Nv + QX) + T_K\}g .$$

### Approximation 2:

Another type of approximation is obtained if we consider both  $g$  and  $h$  in equation (A-19) to be small. In the simpler of these terms in  $gh$ ,  $g^2$ ,  $g^3$ ,  $g^2h$  and  $gh^2$  are all neglected, then the expressions for  $B_2$ ,  $B_1$  and  $B_0$  become,

$$B_2 = B - Q ,$$

$$B_1 = Q(P + Nv + QX) - (Pv + R_X - S_K) + BR ,$$

$$B_0 = \{R(Pv + R_X - S_K) + T_K\} - \{R(P + Nv + QX) + T_K\}g .$$

It may be noted that the coefficient  $B_2$  differs from that of approximation 1 and that approximation 2 is somewhat more accurate. A further approximation can be obtained by neglect of the third order terms only.

### Approximation 3:

Yet another type of approximation is obtained by considering  $g$  only as small. If in the expressions for  $B_2$ ,  $B_1$  and  $B_0$  terms in  $g^2$  and  $g^3$  are neglected, we obtain,

$$B_2 = B - Q - g ,$$

$$B_1 = \{Q(P + Nv + QX) - (Pv + R_X - S_K) + BR\} - (BQ - 2R)g ,$$

$$B_0 = \{R(Pv + R_X - S_K) + T_K\} - \{R(P + Nv + QX) + T_K\}g .$$

In this form  $B_2$  is exact and  $B_1$  is an improved approximation. If only terms in  $g^3$  are neglected then  $B_1$  takes on its exact form and  $B_0$  only differs from its exact value by  $-Rg^3$ .

In Fig 7, approximation 1 is used to obtain values of  $h$  and  $g$  for comparison with the exact.

#### A.6 Effect of varying $\kappa$ on the stability of the Spitfire V

In Ref 4 the coefficients of the longitudinal stability quartic for the Spitfire V are quoted as functions of  $\omega$  and  $\kappa$ . We now consider the locus of  $g, h$  for varying  $\kappa$  at four levels of  $\omega, C$  or  $H_m$ . Thus in Fig 8,  $\omega = -7.035$ ,  $H_m = -0.005$ . With this negative manoeuvre margin the aircraft is statically stable when  $\kappa \leq -0.224$  ( $K_n > 0$ , see Fig 8). However it falls within the unstable oscillation region for values of  $\kappa < -0.66$  (or  $K_n > 0.05$  approximately). Between  $K_n = 0$  and  $K_n \approx 0.05$  the motion consists of two divergences. In fact the phugoid motion is only stable when the static margin is more negative than about  $-0.007$ .

Approximate values of the static margin  $K_n$  are marked alongside the curve. As remarked elsewhere variation of  $\kappa$  for fixed  $\omega$  is equivalent to the variation of  $K_n$  for fixed  $H_m$ .

The next figure (Fig 9) shows similar trends for the case of the aircraft with zero manoeuvre margin. With manoeuvre margins of 0.01 and 0.05 the locus over the range of  $K_n$  of  $-0.2$  to  $+0.2$  does not depart much from the linear approximation, see Fig 10. However for  $H_m = 0.01$  and  $K_n \approx -0.2$  the approximate values of  $g$  and  $h$  are appreciably in error.

Thus far we have been concerned, in the main, with the locus of  $g, h$  in the neighbourhood of some chosen datum. To each point of the curve there corresponds a value of  $\kappa$  (and hence  $K_n$ ) as given by equations (A-6) and (A-7) and the values of  $K_n$  along the curves of Figs 8, 9 and 10 are determined approximately by interpolation of the  $\kappa$  values. When the point  $g, h$  (or the corresponding point  $G, H$ ) represents an oscillation no difficulty arises in the calculation of  $\kappa$ . However when all roots are real ambiguity can arise as discussed in section 6. To illustrate the point we consider that part of the locus in Fig 8 which lies below the curve  $g^2 = 4h$ . This is reproduced in Fig 11. Since the points between A and B on the locus of  $g, h$  and the points between the corresponding points A' and B' of the  $G, H$  locus represent real roots of the quartic, there are six combinations of these roots. These appear as sets of three points on each curve as indicated in Fig 11. Apart from the fact that the values of  $\kappa$  must be in sequence as the chosen point moves from A to B, there seems to be no other way of discriminating between the alternatives unless a one-parameter stability diagram is prepared (cf Figs 13 to 15).

It is of interest to examine the trends for large positive and large negative values of the parameter  $\kappa$ . For numerically large values of  $g$  we may approximate to equation (A-4) as follows,

$$\frac{S}{T} = \kappa = \frac{-g^3}{h^2 - g^2 h} \quad (A-21)$$

that is

$$kh^2 - kg^2h + g^3 = 0 \quad (A-22)$$

The solution of equation (A-22) is

$$h = g^2 \quad \text{or} \quad \frac{g}{k} \quad (A-23)$$

These limiting forms of the curves are sketched in Fig 12.

To relate the value of  $g$  to the trend in  $\kappa$  we note that for large  $g$ ,

$$gh \rightarrow \frac{1}{2}(S\kappa + g^3) \quad (A-24)$$

When equations (A-23) and (A-24) are combined we have,

$$g^3 \rightarrow \pm S\kappa \quad (A-25)$$

The two solutions in equations (A-23) and (A-25) refer to the  $g, h$  locus and the  $G, H$  locus respectively, if these are identified with the 'phugoid' factor and the 'short period' factor. This is arbitrary and to emphasise this the curves of Fig 12 are marked with a dual interpretation.

#### A.7 Locus of $g, h$ as $\omega$ is varied (Spitfire V)

If, in the data for the Spitfire V as listed earlier, we fix  $\kappa$  at -0.085 the coefficients of the stability quartic become functions of  $\omega$  as do the two margins  $K_n$  and  $H_m$ . To trace the locus of  $g, h$  as  $\omega$  is varied equation (A-5), or its equivalent equation (A-19), is used to evaluate  $h$  for a range of values of  $g$ . The locus is a closed curve approximately elliptical in shape, see Appendix B. Along the arc ABC of this curve the values of  $\omega$  as given by equations (A-8) or (A-9) are not necessarily unique, as it turns out that all four roots of the quartic are real in this range. Accordingly there are three values of  $g$  and  $h$  corresponding to a given  $\omega$  in the range affected as illustrated by the points for  $\omega = -3$  and  $-4$  in Fig 13a&b.

A portion of the locus is shown enlarged in Fig 13b, so as to enable approximate values of  $\omega$  to be marked along the curve. The point  $\omega = \pm\infty$  is given by  $g = Q = 0.03039$  and  $h = R = 0.002357$ . Also plotted in Fig 13a is the locus of  $g, h$  when the value of  $\kappa$  is changed to  $-0.127$ . It also passes through the same point for  $\omega = \pm\infty$ , as would the whole family of curves for different  $\kappa$ . For points between C and A the factor  $\lambda^2 + \lambda g + h$  represents a stable oscillation, see Fig 13.

In the next figure (Fig 14) the locus of  $G, H$  (the 'short period' factor coefficients) is plotted. On it are indicated the points corresponding to A and C of the curve in Fig 13 and the boundary  $G^2 = 4H$  (cf Fig 1). The points for  $\omega = -3$  and  $-4$  would number three in all, corresponding to different combinations in pairs of the four real roots, of which only one each is shown.

The minimum value of  $G$  corresponds to  $B - g_{\max}$ , where  $g_{\max}$  is the maximum value of  $g$ . At the value of  $G$  given by  $(B - Q)$ ,  $\omega \rightarrow \pm\infty$  and the locus becomes asymptotic to the line  $G = B - Q$ . On the basis of the results obtained a one-parameter stability diagram may be prepared. This entails solution of two quadratics and as explained previously no difficulty arises when either quadratic represents an oscillation. However between  $\omega = -4.914$  and  $-2.60$  the quartic has four real roots and it is necessary to proceed in the following manner to relate these to a certain value of  $\omega$ . For a point of the  $g, h$  locus (along ABC) determine the value of  $\omega$  and the corresponding value of  $G = B - g$ . With this value of  $G$  we solve for  $H$  and accept the value of  $H$  which yields the same value of  $\omega$  as given by the point  $g, h$ . Thus the curves of Figs 13 and 14 contain the information of the many curves of Fig 15.

As  $\omega \rightarrow \pm\infty$  the quartic factorizes approximately as  $\{\lambda^2 + (B - Q)\lambda + \omega\} \times \{\lambda^2 + Q\lambda + R\}$ , a result which follows easily by inspection or from the equations (A-5), (A-8) and (A-9).

#### A.8 Locus of $g, h$ for varying $\omega$ , all other parameters constant, for the aircraft of R&M 2078

In Ref 11 Neumark tabulates the roots of the longitudinal stability quartic for an aircraft of specified characteristics over a wide range of  $\omega$ ,  $-2$  to  $+\infty$ . The results are also displayed in the form of a one-parameter stability diagram. It is, therefore, interesting to examine the locus of  $g, h$  and  $G, H$  for this aircraft as given by the present method.



In Fig 16 the coefficients  $g, h$  as derived from Neumark's results and further values as obtained by application of equation (A-19) are plotted. Neumark's results identify the point A as corresponding to  $\omega = 0.2369$  in agreement with a value of  $\omega = 0.2367$  from equation (A-9). Since he calculated the roots for the two negative values of  $\omega = -1.0$  and  $-2.0$  on the arc ABA' it seems that he might have attempted to locate A', the other point of intersection with the curve  $g^2 = 4h$ , but failed to hit on the appropriate value of  $\omega$ . Points on the locus above A' correspond to the third type of oscillation arising from a recombination of two real roots, cf Fig 15. The locus is to a close approximation an ellipse as indicated in Fig 16.

To obtain the corresponding G, H locus equation (A-19) is used to calculate H for a range of values of G in the neighbourhood of  $G = B - Q$ , the asymptotic value of G as  $\omega \rightarrow \pm\infty$ . When the coordinates so obtained and those derived from Neumark's results are plotted the curve of Fig 17 is obtained.

#### A.9 Analysis of the stability of the Spitfire V aircraft in terms of its static and manoeuvre margin values

Since the static margin is linearly related to the parameters  $\omega$  and  $\kappa$  and the manoeuvre margin to the parameter  $\omega$ , we may write the coefficients of the quartic in terms of the margins  $K_n$  and  $H_m$ , as follows,

$$\begin{aligned} B &= 6.010, \\ C &= 291.37529H_m + 0.16108, \\ D &= 8.69050H_m + 0.15685K_n - 0.04744, \\ E &= 0.65525K_n. \end{aligned}$$

These enable the stability of the aircraft to be examined using equations (A-13) and (A-14) when  $K_n$  is varied, for fixed  $H_m$  and  $H_m$  is varied, for fixed  $K_n$ , respectively.

##### A.9.1 Locus of $g, h$ for varying $K_n$ , fixed $H_m$

As already remarked the variation of  $K_n$  with a fixed value of  $H_m$ , the manoeuvre margin, is equivalent to variation of  $\kappa$  with  $\omega$  held fixed. Accordingly the curves of Figs 8 to 10 are marked with the values of  $K_n$  and the fixed value of  $H_m$  indicated on each diagram and are capable of the dual interpretation.

### A.9.2 Locus of $g, h$ for varying $H_m$ , fixed $K_n$

To fix the value of  $K_n$ , the static margin, is to establish a linear relationship between  $\omega$  and  $\kappa$ . Hence as  $H_m$  (or  $\omega$ ) is varied the value of  $\kappa$  changes to retain the constant  $K_n$ , static margin. With  $K_n = 0.05$  the locus of  $g, h$  for varying  $H_m$  as given by equation (A-14) is the curve shown in Fig 18. It follows from equation (A-14) that as  $h \rightarrow \pm 0$ ,  $g \rightarrow 0.0298$  and using the associated equations for  $H_m$  it can be seen that  $H_m \rightarrow \pm \infty$ .

By use of the same equation it is possible to construct the locus of  $G, H$ , the coefficients of the other quadratic factor of the stability quartic. This is illustrated in Fig 19 where it can be seen that  $G = B - 0.0298$  is an asymptote. This corresponds to the point 0.0298, 0 of Fig 18. The result can be readily derived by approximate factorization of the quartic as  $H_m \rightarrow \infty$ . The quartic becomes approximately

$$\lambda^4 + B\lambda^3 + C_m H_m \lambda^2 + D_m H_m \lambda + E_n K_n = 0,$$

which factorizes into

$$\left\{ \lambda^2 + \left( B - \frac{D_m}{C_m} \right) \lambda + C_m H_m \right\} \left\{ \lambda^2 + \frac{D_m}{C_m} \lambda + \frac{E_n K_n}{C_m H_m} \right\} = 0.$$

That is,

$$G \rightarrow B - \frac{D_m}{C_m}, \quad H \rightarrow C_m H_m \rightarrow \pm \infty$$

and

$$g \rightarrow \frac{D_m}{C_m}, \quad h \rightarrow \pm 0.$$

The curves of Figs 18 and 19 cover the range of practical interest, but the fact that curves are not bounded in the same way as the curves for varying  $\omega$  is of interest and merits further consideration.

Equation (A-14) can be written as

$$C_2 h^2 + C_1 h + C_0 = 0$$

$$\text{where } C_2 = B - g - \frac{D_m}{C_m},$$

$$C_1 = \frac{D_m}{C_m} g^2 - B \frac{D_m}{C_m} g + \frac{D_m}{C_m} \{P + (N - \frac{1}{2} C_{L\alpha})v + QX\} \\ - D_n K_n - \left\{ P + \left( C_L + \frac{V}{2} \frac{\partial C_L}{\partial V} \right) S \right\} v - RX,$$

$$C_0 = E \left( g - \frac{D_m}{C_m} \right).$$

For large values of  $g$  the coefficients  $C_2$ ,  $C_1$  and  $C_0$  are given approximately by,

$$C_2 \approx -g$$

$$C_1 \approx cg(g - B)$$

$$C_0 \approx Eg,$$

where  $c = D_m/C_m$ . This gives a quadratic to which the solution is,

$$h \approx c(g - B) \quad \text{or} \quad -\frac{E}{c(g - B)}.$$

Thus in the limit  $h$  behaves as either  $cg$  or  $-(E/cg)$  ( $E > 0$ ,  $c > 0$ ). If we identify  $g$ ,  $h$  with a point on the branch of the curve of Fig 18 that refers to the 'phugoid' factor, then we are interested in the behaviour of  $h$  as  $g \rightarrow -\infty$ . It follows from the result just given that  $h \rightarrow -\infty$  or  $+0$ , and that  $H_m \rightarrow -\infty$  in both cases. When  $g \rightarrow -\infty$ ,  $G \rightarrow +\infty$  since  $G + g = B$ . By virtue of the solution to the quadratic, which applies equally to  $G$  and  $H$ , we have  $H \rightarrow +\infty$ ,  $-0$ , whilst again  $H_m \rightarrow -\infty$ . The curves of Figs 18 and 19 show that for  $H_m \rightarrow -\infty$  the quartic has four real roots and so coefficients  $g$ ,  $h$  and  $G$ ,  $H$  appear three times on each curve for  $H_m \rightarrow -\infty$ , corresponding to the six different combinations of the roots in pairs. It is possible to derive the same result by direct approximate factorization of the quartic. For large  $H_m$  the quartic is approximately,

$$\lambda^4 + B\lambda^3 + C_m H_m \lambda^2 + D_m H_m \lambda + E = 0$$

which factorizes into

$$\left\{ \lambda^2 + \left( B - \frac{D_m}{C_m} \right) \lambda - k^2 \right\} \left\{ \lambda^2 + \frac{D_m}{C_m} \lambda - \frac{E}{k^2} \right\} = 0$$

where  $C_m H_m = -k^2$ ,  $k$  large and positive. Thus the four real roots of the quartic as  $H_m \rightarrow -\infty$  are

$$(a) \quad \lambda = k + \frac{1}{2} \left( \frac{D_m}{C_m} - B \right),$$

$$(b) \quad \lambda = -k + \frac{1}{2} \left( \frac{D_m}{C_m} - B \right),$$

$$(c) \quad \lambda = -\frac{D_m}{C_m},$$

$$(d) \quad \lambda = \frac{EC_m}{D_m k^2} \text{ approximately.}$$

If we assume  $k$  positive,

$$(a) \text{ and } (b) \text{ yield the point } G = B - \frac{D_m}{C_m}; \quad H \rightarrow -\infty$$

$$(b) \text{ and } (c) \text{ yield the point } G \rightarrow k \rightarrow +\infty; \quad H \rightarrow \frac{kD_m}{C_m} \rightarrow +\infty$$

$$(b) \text{ and } (d) \text{ yield the point } G \rightarrow k \rightarrow +\infty; \quad H \rightarrow -\frac{EC_m}{D_m k} \rightarrow -0$$

$$(a) \text{ and } (c) \text{ yield the point } g \rightarrow -k \rightarrow -\infty; \quad h \rightarrow -\frac{D_m k}{C_m} \rightarrow -\infty$$

$$(a) \text{ and } (d) \text{ yield the point } g \rightarrow -k \rightarrow -\infty; \quad h \rightarrow \frac{EC_m}{D_m k} \rightarrow +0$$

$$(c) \text{ and } (d) \text{ yield the point } g \rightarrow \frac{D_m}{C_m}; \quad h \rightarrow -\frac{E}{k^2} \rightarrow -0.$$

This explains the trends exhibited by the curves of Fig 20.

The difference between the closed, compact nature of the curves of Figs 13 and 16 as compared with that of Fig 20 underlines the essentially approximate nature of the manoeuvre margin as a system parameter. In contrast, the concise quantity  $\omega$  is a natural system parameter.

# Appendix B

## SOME REMARKS ON THE GEOMETRY OF THE LOCUS OF $g, h$

A look at the approximations to the various loci to a second order in  $g$  and  $h$  (the resulting curves are then conics) helps to establish the nature of the curves generally.

### B.1 Locus of $g, h$ for varying $\kappa$ (second-order approximation)

From equation (A-4) we have, to second-order in  $g$  and  $h$

$$\begin{aligned} \frac{S}{T} h^2 + \left( B \frac{S}{T} - 2 \right) gh - Bg^2 + (\omega + P + Nv + QX)g \\ + \left\{ B - \frac{S}{T} (\omega + P + Nv + QX) \right\} h + \left( R \frac{S}{T} - Q \right) \omega + Pv + RX = 0 . \end{aligned}$$

The nature of this conic is determined by

$$- B \frac{S}{T} - \frac{1}{4} \left( B \frac{S}{T} - 2 \right)^2 = - \frac{1}{4} \left( \frac{B^2 S^2}{T^2} + 4 \right) < 0 .$$

Hence the curve is a hyperbola to this degree of approximation.

### B.2 Locus of $g, h$ for varying $\omega$ (linear approximation of equation (A-20))

The equation to the curve according to approximation I (see equation (A-20)) is

$$\begin{aligned} Bh^2 + \{ Q(P + Nv + QX) - (Pv + RX - S\kappa) + BR \} h \\ + \{ R(Pv + RX - S\kappa) + T\kappa \} - \{ R(P + Nv + QX) + T\kappa \} g = 0 . \end{aligned}$$

Since there is no term in  $gh$  or  $g^2$  this is a parabola. Furthermore since the equation to the curve can be written in the form,

$$B(h - h_0)^2 = \{ R(P + Nv + QX) + T\kappa \} (g - g_0) ,$$

the axis of the parabola is parallel to the  $h = 0$  axis.

### B.3 Locus of g, h for varying $\omega$ (quadratic approximation of equation (A-20))

The equation to the curve in this case is

$$B_2 h^2 + B_1 h + B_0 = 0 ,$$

where  $B_2 = B - Q$  ,

$$B_1 = Q(P + Nv + QX) - (Pv + R\chi - S\kappa) + BR - (BQ - 2R)g ,$$

$$B_0 = \{R(Pv + R\chi - S\kappa) + T\kappa\} - \{R(P + Nv + QX) + T\kappa\}g + BRg^2 .$$

This is the next higher order approximation mentioned in Appendix A, section A.5 (approximation 2).

Here the coefficients of  $h^2$ ,  $gh$  and  $g^2$  are as follows,

$$h^2 : B - Q$$

$$gh : 2R - BQ$$

$$g^2 : BR ,$$

and the test function for the conic is

$$BR(B - Q) - \frac{1}{4} (2R - BQ)^2 = B^2 \left( R - \frac{Q^2}{4} \right) - R^2 .$$

But,

$$R = \frac{C_{Le}}{2} \left( C_L + \frac{v}{2} \frac{\partial C_L}{\partial V} \right)_e$$

$$Q = \left( C_D + \frac{v}{2} \frac{\partial C_D}{\partial V} \right)_e .$$

If the change with speed of  $R$  and  $Q$  is negligible or absent then  $R = \frac{1}{2} C_{Le}^2$  ,  $Q = C_{De}$  and the test function for the conic becomes,

$$\frac{1}{4} \left\{ B^2 (2C_L^2 - C_D^2)_e - C_{Le}^4 \right\} ,$$

which is usually  $> 0$  , so that the curve is an ellipse.

LIST OF SYMBOLSMain text

$\bar{c}$	mean chord of wing
$C_D$	drag coefficient = $D/\frac{1}{2}\rho V^2 S$
$C_L$	lift coefficient = $L/\frac{1}{2}\rho V^2 S$
$D$	drag
$g$	coefficient of $\lambda$ in quadratic factor
$G$	coefficient of $\lambda$ in quadratic factor
$h$	constant term in quadratic factor
$H$	constant term in quadratic factor
$H_m$	manoeuvre margin
$iy$	inertia parameter = $I_y/m_e \bar{c}^2$
$I_y$	moment of inertia about y-axis
$K_0, K_1, K_2, K_3, K_4$	coefficients of the stability quartic
$K_n$	static margin
$L$	lift
$m_e$	aircraft mass in equilibrium flight
$\left. \begin{array}{l} m_q \\ m_u \\ m_w \\ m_{\dot{w}} \end{array} \right\}$	concise moment quantities, see R&M 3562 or ESDU data items
$Q$	kinetic pressure = $\frac{1}{2}\rho V^2$
$R$	Routh's discriminant
$Q$ with suffix	polynomial involved in coefficients of stability quartic
$u$	component of aircraft velocity along x-axis
$U$ with suffix	polynomial involved in coefficients of stability quartic
$V$	resultant velocity of aircraft
$w$	component of aircraft velocity along z-axis
$W$ with suffix	polynomial involved in coefficients of stability quartic



LIST OF SYMBOLS (continued)

$\left. \begin{array}{l} x_u \\ x_w \\ x_w^\bullet \\ z_q \\ z_u \\ z_w \\ z_w^\bullet \end{array} \right\}$	concise force quantities, see R&M 3652 or ESDU data items
$\alpha$	angle of attack
$\lambda$	root of the stability quartic
$\mu_l$	relative density parameter = $m_e / \frac{1}{2} \rho_e S \bar{c}$
$\rho$	air density
<u>Appendices A and B</u> (cf R&M 2027 and R&M 2078)	
B, C, D, E	coefficients of stability quartic
$C_{AS}$	propeller contribution to $x_u$ derivative = $[(-1/\rho S V)(\partial T/\partial V)]_e$ , propeller 'drag' coefficient
$C_{L\alpha}$	rate of change of $C_L$ with $\alpha = \partial C_L / \partial \alpha$
$i_B$	inertia parameter = $I_B / m_e \ell^2$
$I_B$	moment of inertia about y-axis
$\ell$	tail arm (distance from cg to mean $\frac{1}{4}$ -chord point of the tailplane)
N	$(\frac{1}{2} C_{L\alpha} + \frac{1}{2} C_D + C_{AS})_e$
P	$\frac{1}{2} \left[ (C_D + C_{AS})(C_{L\alpha} + C_D) + \left( C_L + \frac{1}{2} V \frac{\partial C_L}{\partial V} \right) \left( C_L - \frac{\partial C_D}{\partial \alpha} \right) \right]_e$
Q	$[(C_D + C_{AS}) - \frac{1}{2} C_L \tan \gamma]_e$
R	$\left[ \frac{1}{2} C_L \left\{ C_L + \frac{1}{2} V \frac{\partial C_L}{\partial V} - (C_D + C_{AS}) \tan \gamma \right\} \right]_e$
S	$\frac{1}{2} \left( \frac{\partial C_D}{\partial \alpha} \right)_e$
T	$\left[ \frac{1}{2} C_L \left\{ C_{L\alpha} + C_D + \left( C_L - \frac{\partial C_D}{\partial \alpha} \right) \tan \gamma \right\} \right]_e$

LIST OF SYMBOLS (concluded)

Note: In these expressions the contribution of the  $Z$  force due to rate of pitch has been neglected, cf Table 2 of R&M 2078. In the form given they apply to a propeller driven aircraft at speeds for which compressibility and aeroelastic effects are negligible. In the general case, where compressibility and aeroelastic effects are also included, the  $C_{AS}$  term needs to be replaced by  $C_{AS} + \frac{1}{2}V(\partial C_D/\partial V)$ ,  $C_{AS}$  is zero for a jet-propelled aircraft.

$\gamma$	angle of climb
$\mu$	relative density parameter = $m_e/\rho_e S\ell$
$\kappa$	} concise quantities in the old notation (for relation to concise quantities in the new notation, see R&M 3562, Part 5. For definition in terms of old-notation derivatives, see Refs 4, 5 or 6)
$\nu$	
$\chi$	
$\omega$	

REFERENCES

- | <u>No.</u> | <u>Author</u>              | <u>Title, etc</u>   |
|------------|----------------------------|---|
| 1          | E.J. Routh                 | A treatise on the stability of a given state of motion.<br>Macmillan (1877)   |
| 2          | E.J. Routh                 | Advanced rigid dynamics.<br>Macmillan   |
| 3          | A. Hurwitz                 | Über die Bedingungen, unter welchen eine Gleichung nur<br>Wurzeln mit negativen reellen Teilen besitzt.<br>Math. Ann., <u>46</u> , 273 (1895) |
| 4          | R.A. Frazer<br>W.J. Duncan | On the criteria for the stability of small motions.<br>Proc. Roy. Soc. A, <u>124</u> , 642 (1929)   |
| 5          | W.J. Duncan                | The principles of the control and stability of aircraft.<br>Cambridge University (1952)   |
| 6          | S.B. Gates<br>H.M. Lyon    | A continuation of longitudinal stability and control<br>analysis. Part I - General theory.<br>R&M 2027 (1944)                                 |
| 7          | S. Neumark                 | The disturbed longitudinal motion of an uncontrolled<br>aircraft and of an aircraft with automatic control.<br>R&M 2078 (1943)                |
| 8          | G. Sachs                   | Static stability and aperiodic divergence.<br>Journal of Aircraft, <u>12</u> , 497 (1975)   |
| 9          | A.W. Babister              | Static and dynamic stability.<br>RAeS Aero. Journal, <u>82</u> , 806 (1978)   |
| 10         | H.R. Hopkin                | A scheme of notation and nomenclature for aircraft<br>dynamics and associated aerodynamics.<br>R&M 3562, Parts 1-5 (1970)                     |
| 11         | S. Neumark                 | Problems of longitudinal stability below minimum drag<br>speed and theory of stability under constraint.<br>R&M 2983 (1957)                   |

Fig 1

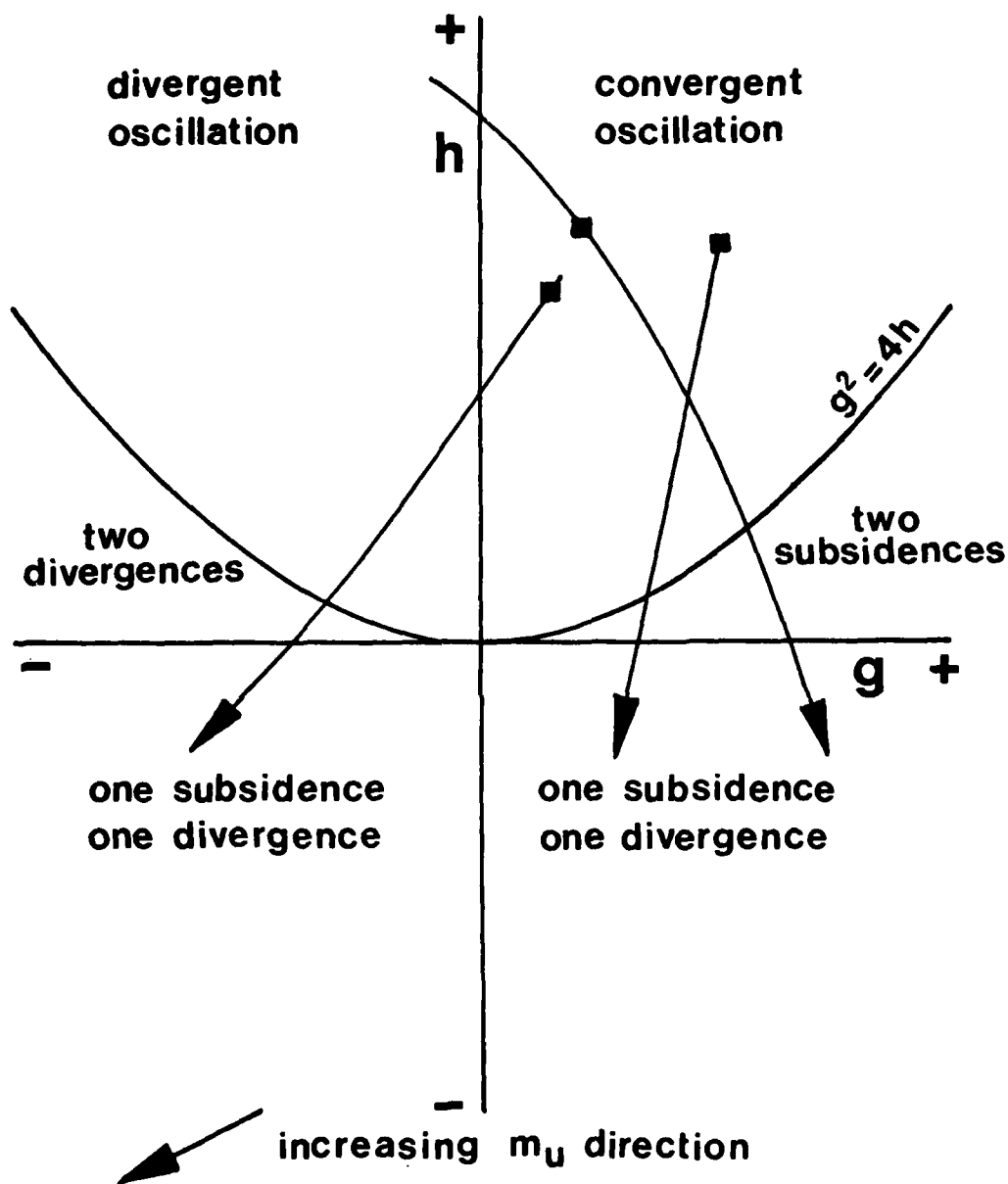


Fig 1 Diagram illustrating analysis of stability using locus of the coefficients  $g, h$  for varying  $m_U$

Fig 2

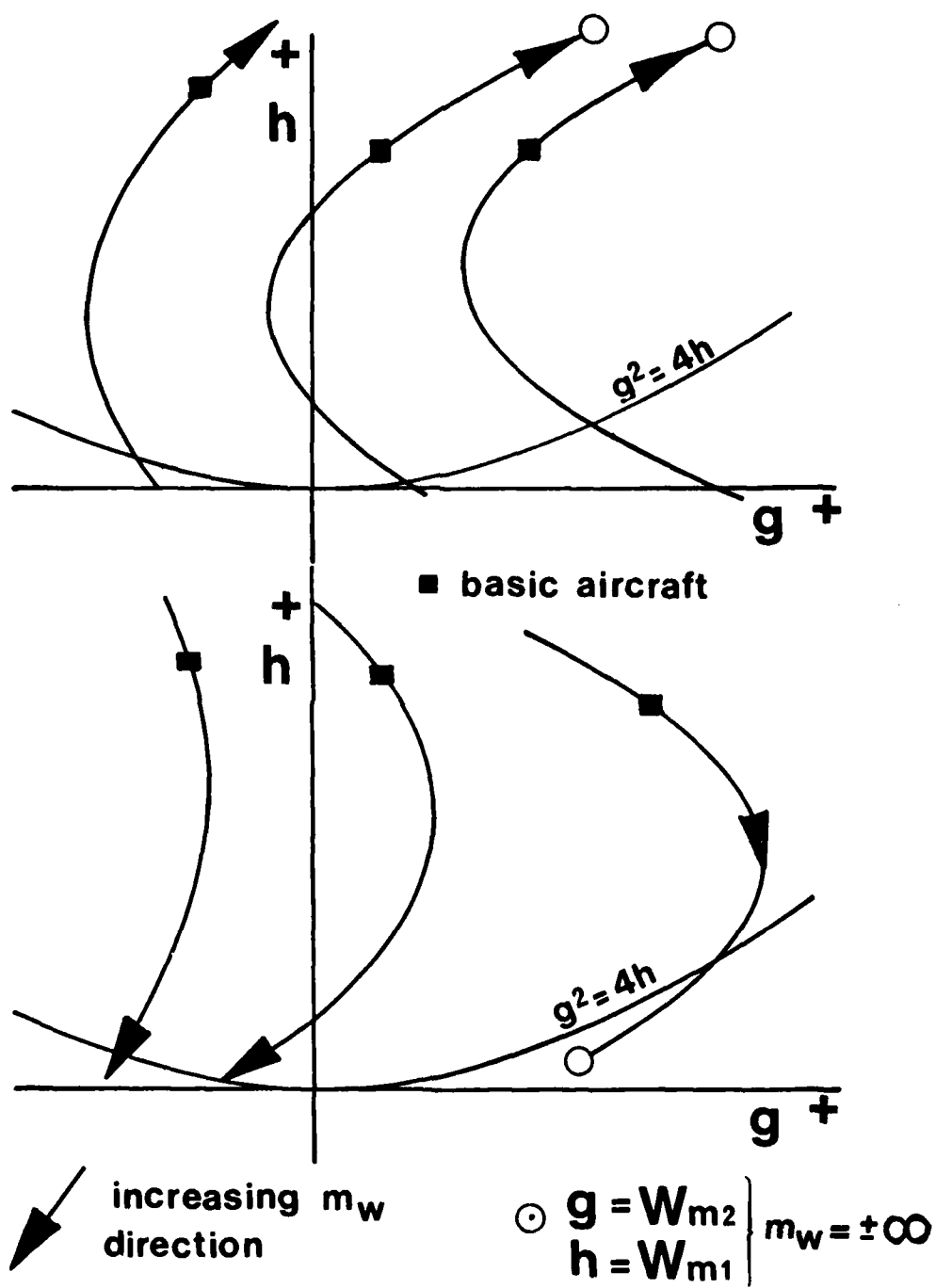


Fig 2 Diagram illustrating analysis of stability using locus of the coefficients  $g, h$  for varying  $m_w$

Fig 3

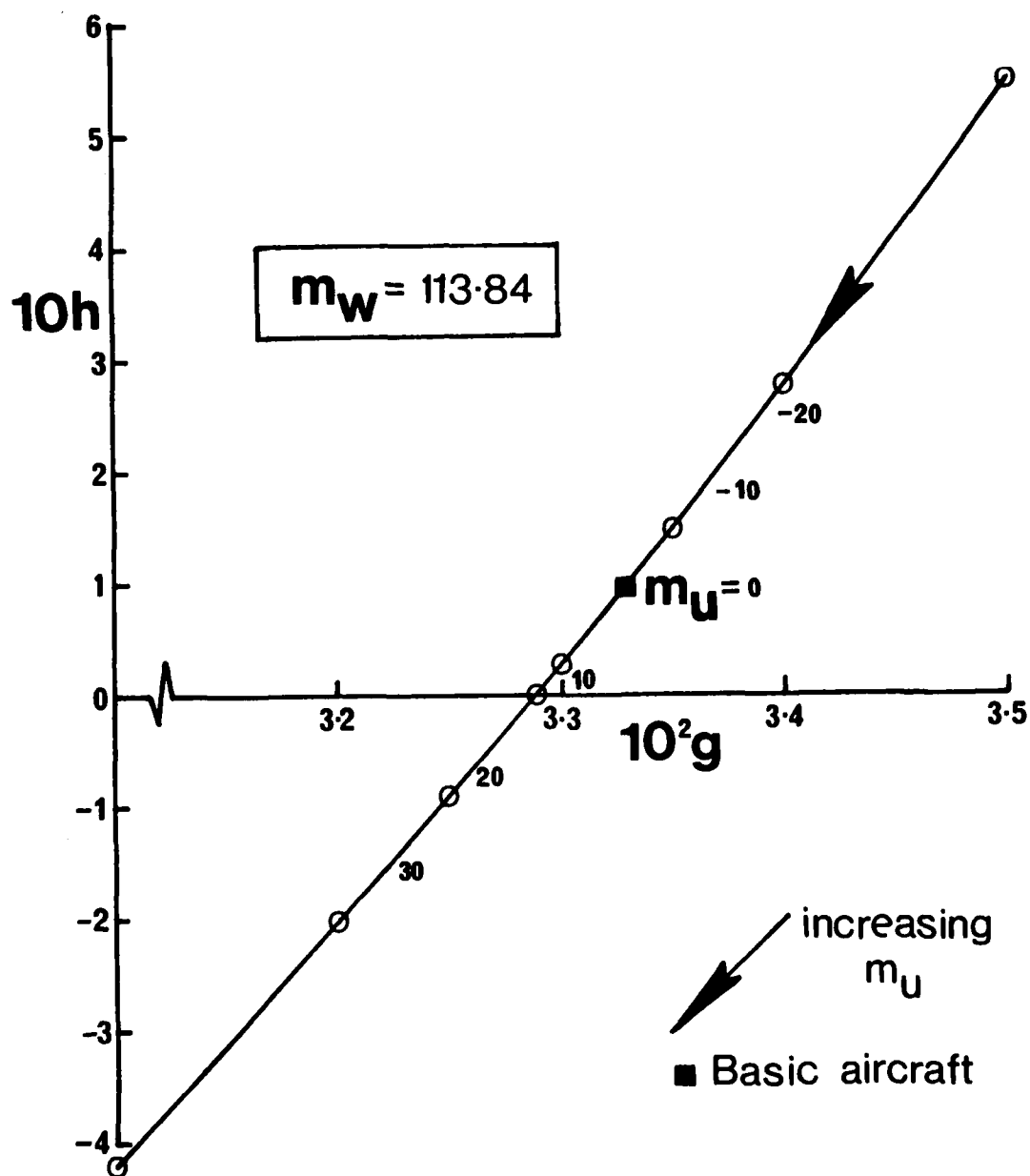
Fig 3 The locus of  $g, h$  as  $m_U$  is varied for the example aircraft of section 5

Fig 4

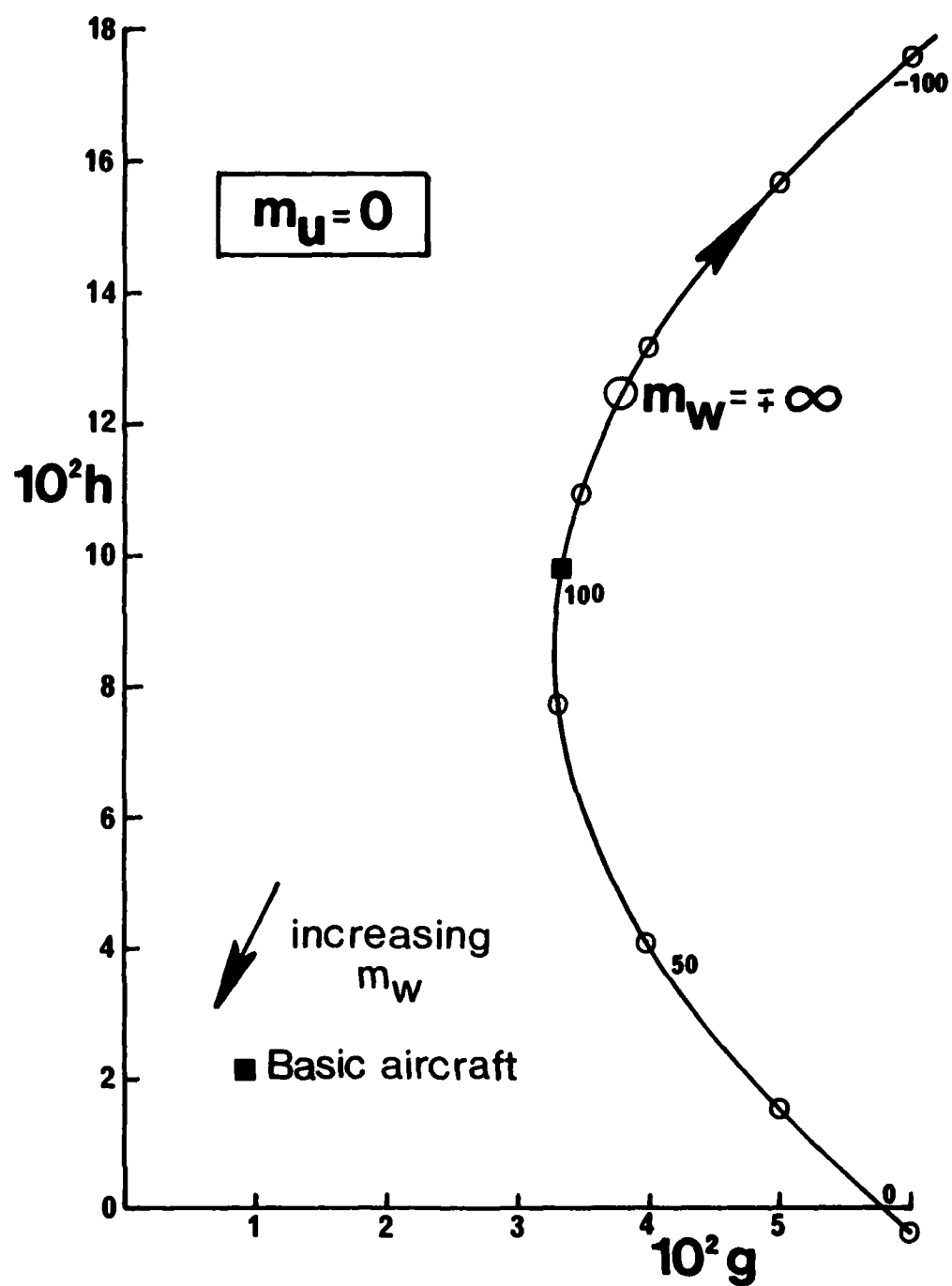


Fig 4 The locus of  $g, h$  as  $m_w$  is varied for the example aircraft of section 5

Fig 5

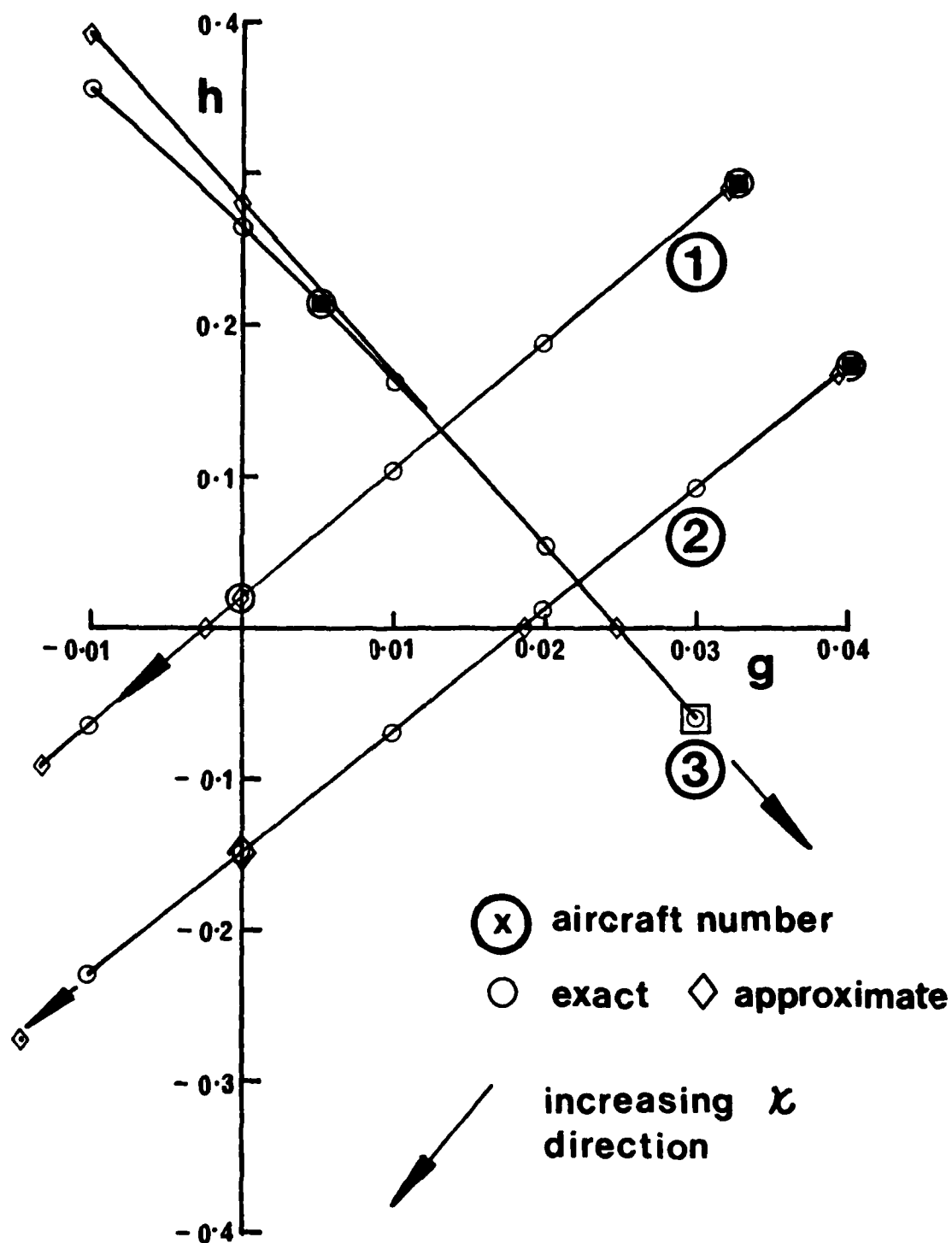
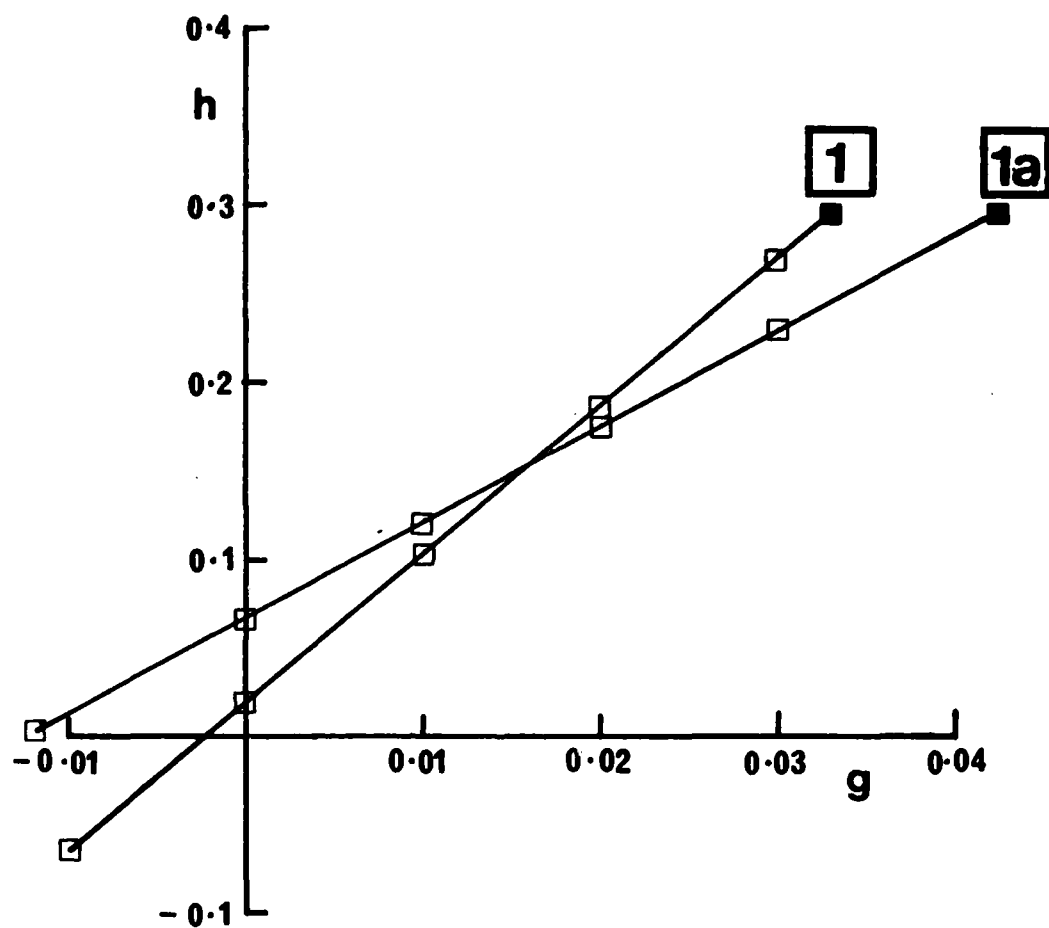


Fig 5 Examples of  $g, h$  locus for varying  $\kappa$  for aircraft 1, 2 and 3 of Appendix A



Fig 6



**1a** aircraft 1 with increased  $\frac{\partial C_D}{\partial C_L}$

Fig 6 Effect of increasing  $\partial C_D / \partial C_L$  on the  $g, h$  locus for varying  $\kappa$  (aircraft 1, see Appendix A)

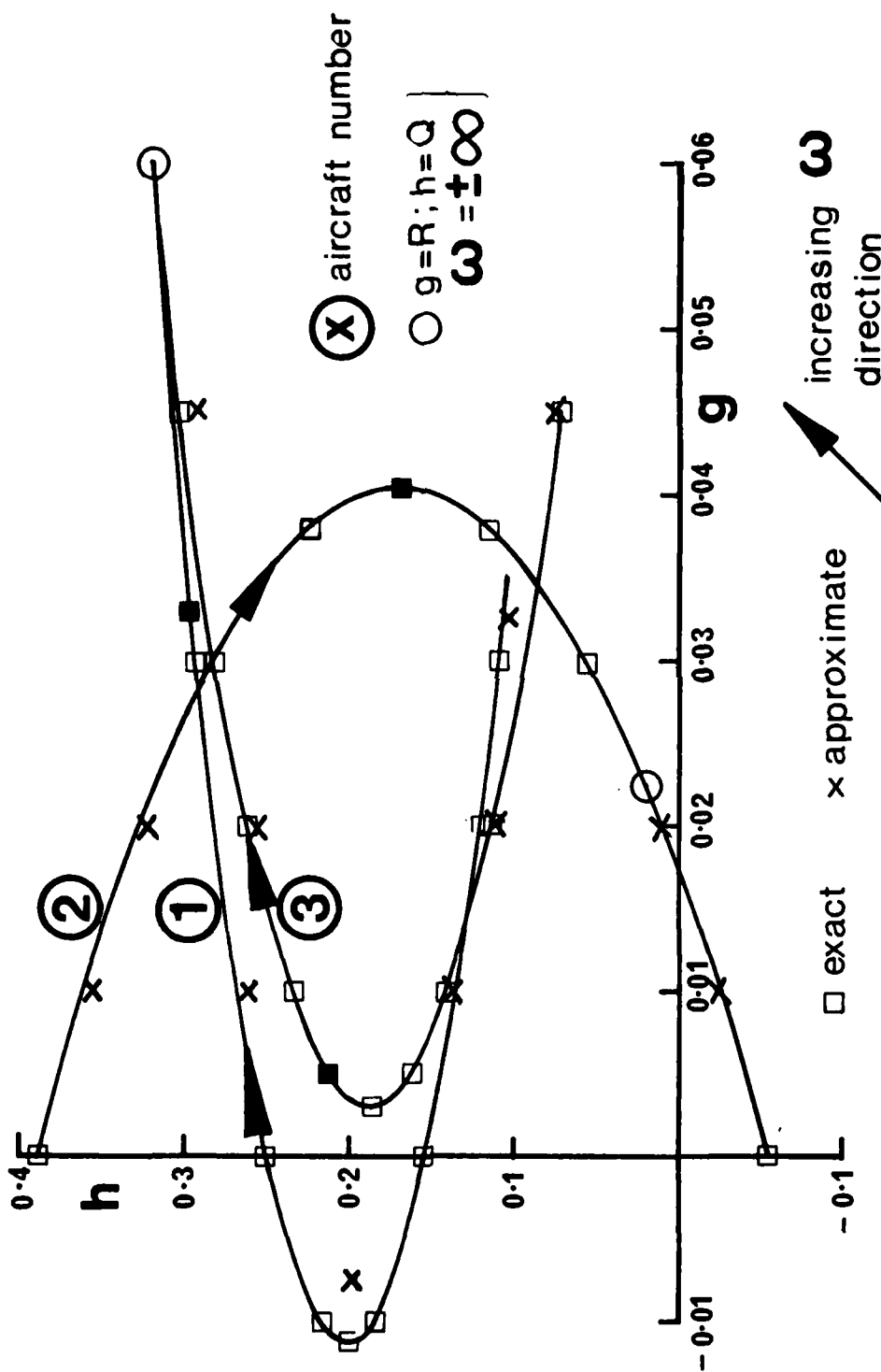


Fig 7 The  $g, h$  locus for varying  $\omega$  (aircraft 1, 2 and 3 of Appendix A)

Fig 8

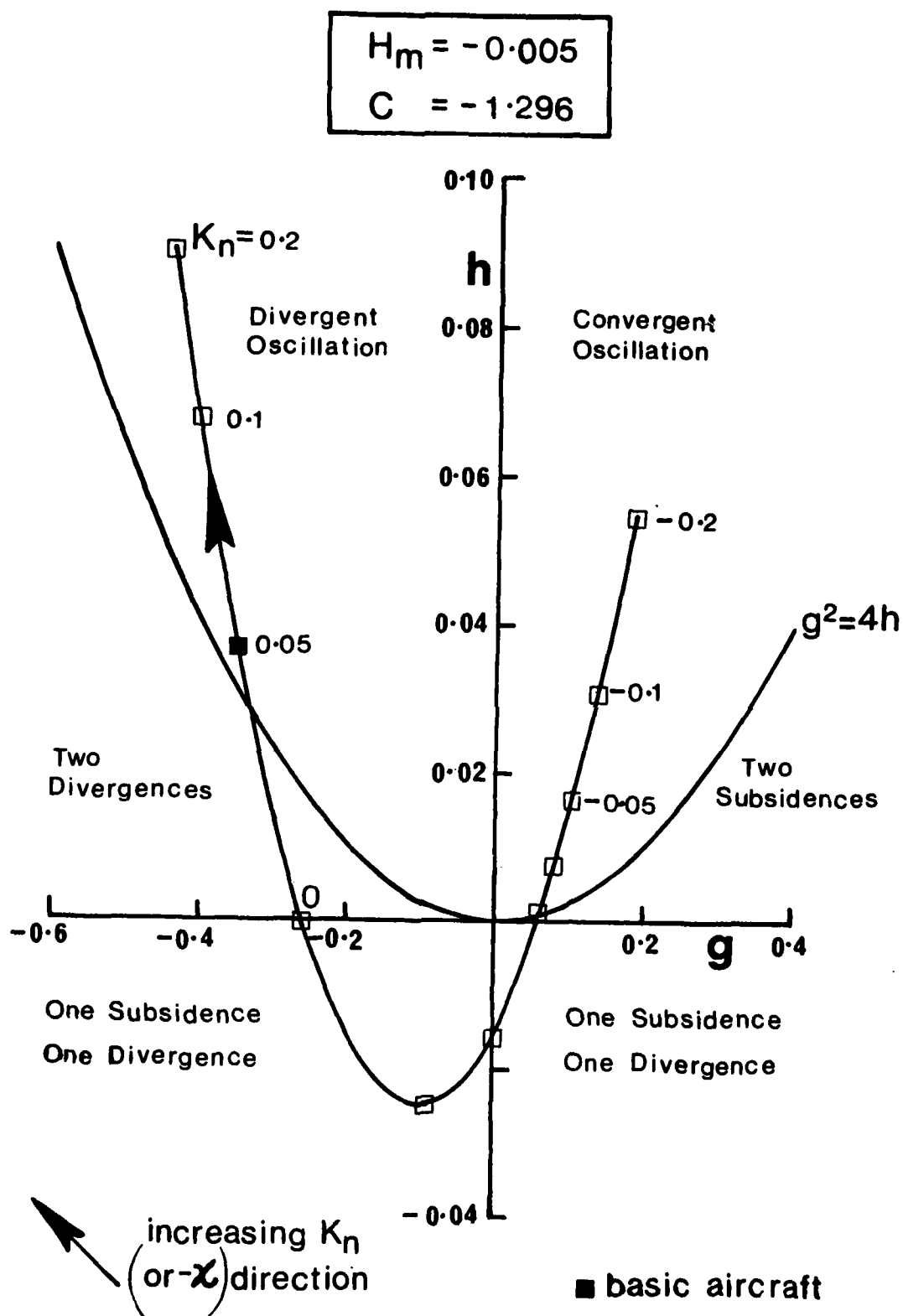


Fig 8 The  $g, h$  locus for varying  $K_n$  or  $\kappa$  ( $\omega$  fixed to give  $H_m = -0.005$ ) (Spitfire V, Ref 6)

Fig 9

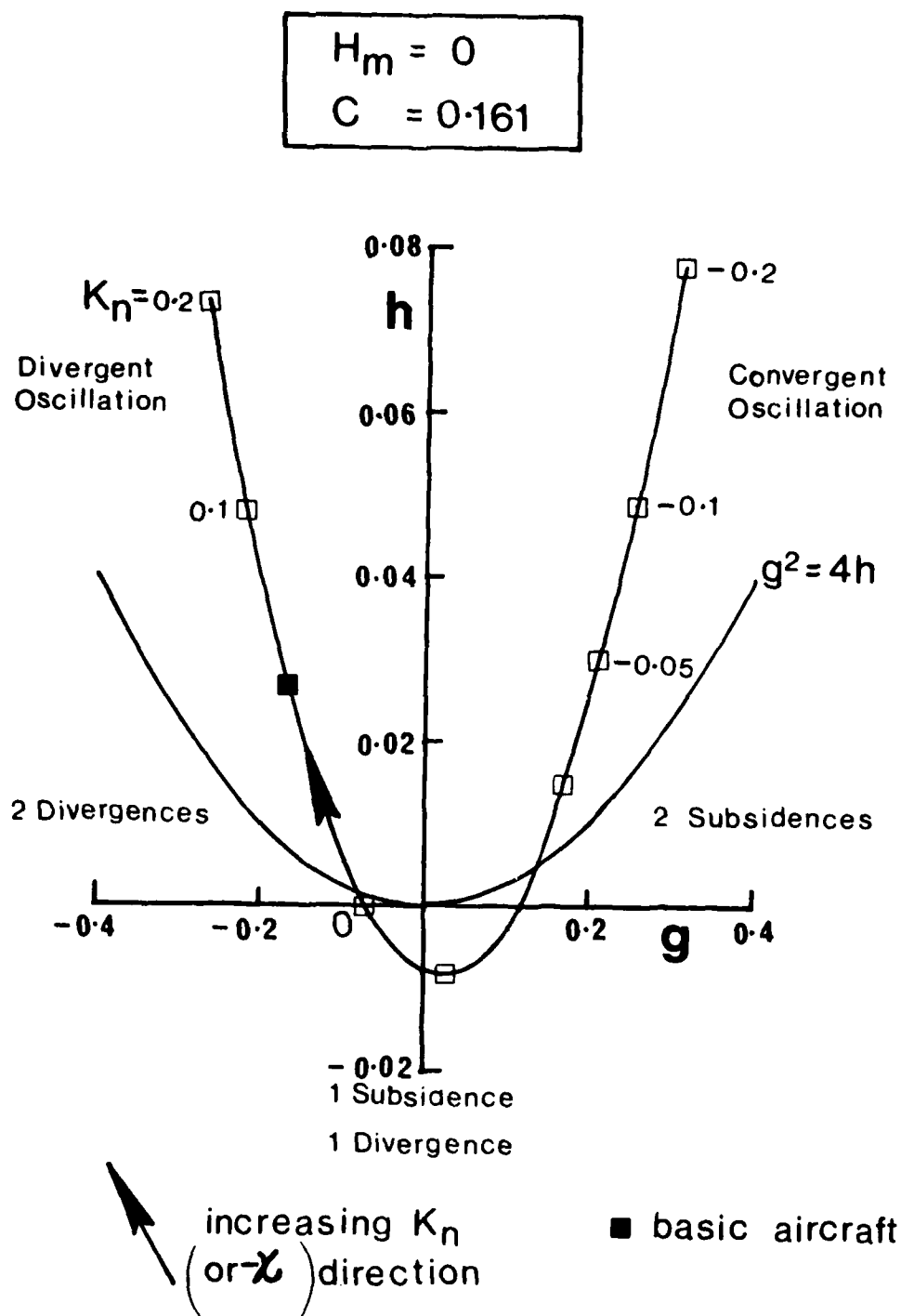


Fig 9 The  $g, h$  locus for varying  $K_n$  or  $\kappa$  (zero manoeuvre margin)  
(Spitfire V, Ref 6)

Fig 10

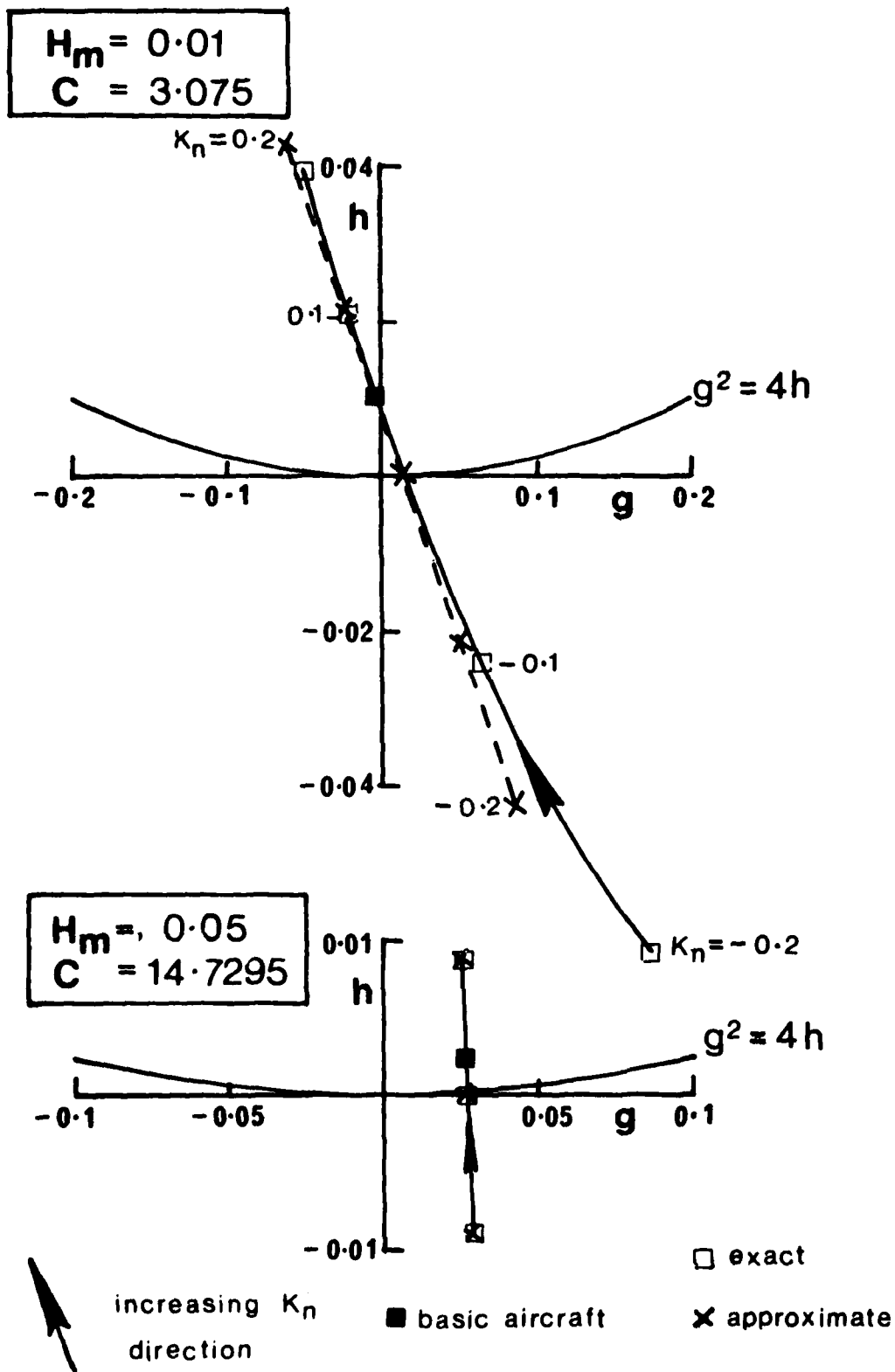


Fig 10 The  $g, h$  locus for varying  $K_n$  or  $\kappa$  ( $H_m = 0.01$  and  $0.05$ )  
 (Spitfire V, Ref 6)

Fig 11a&amp;b

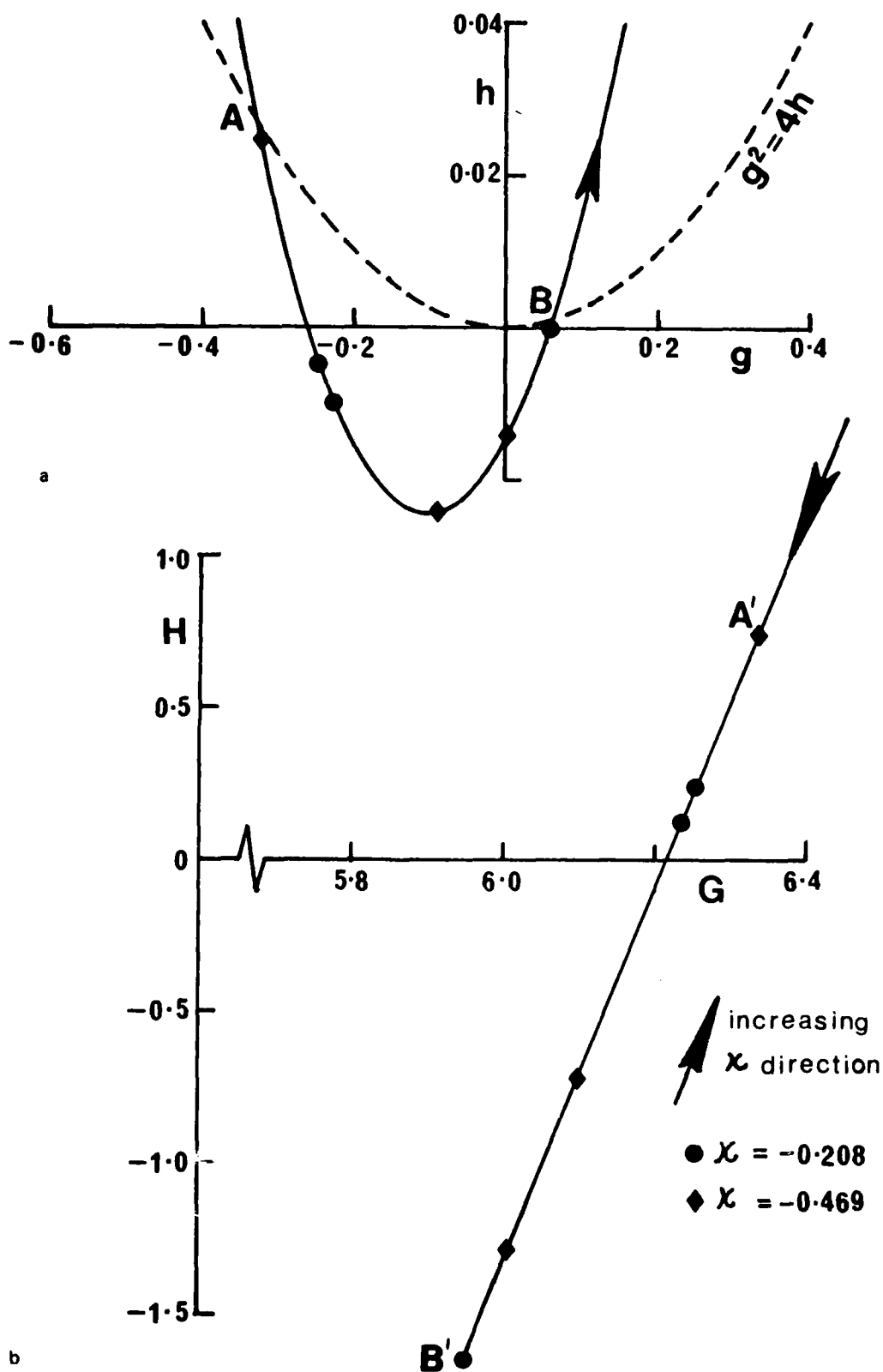


Fig 11a&amp;b Multiple points on locus corresponding to four real roots of the stability quartic (cf Figs 8 and 12)

Fig 12

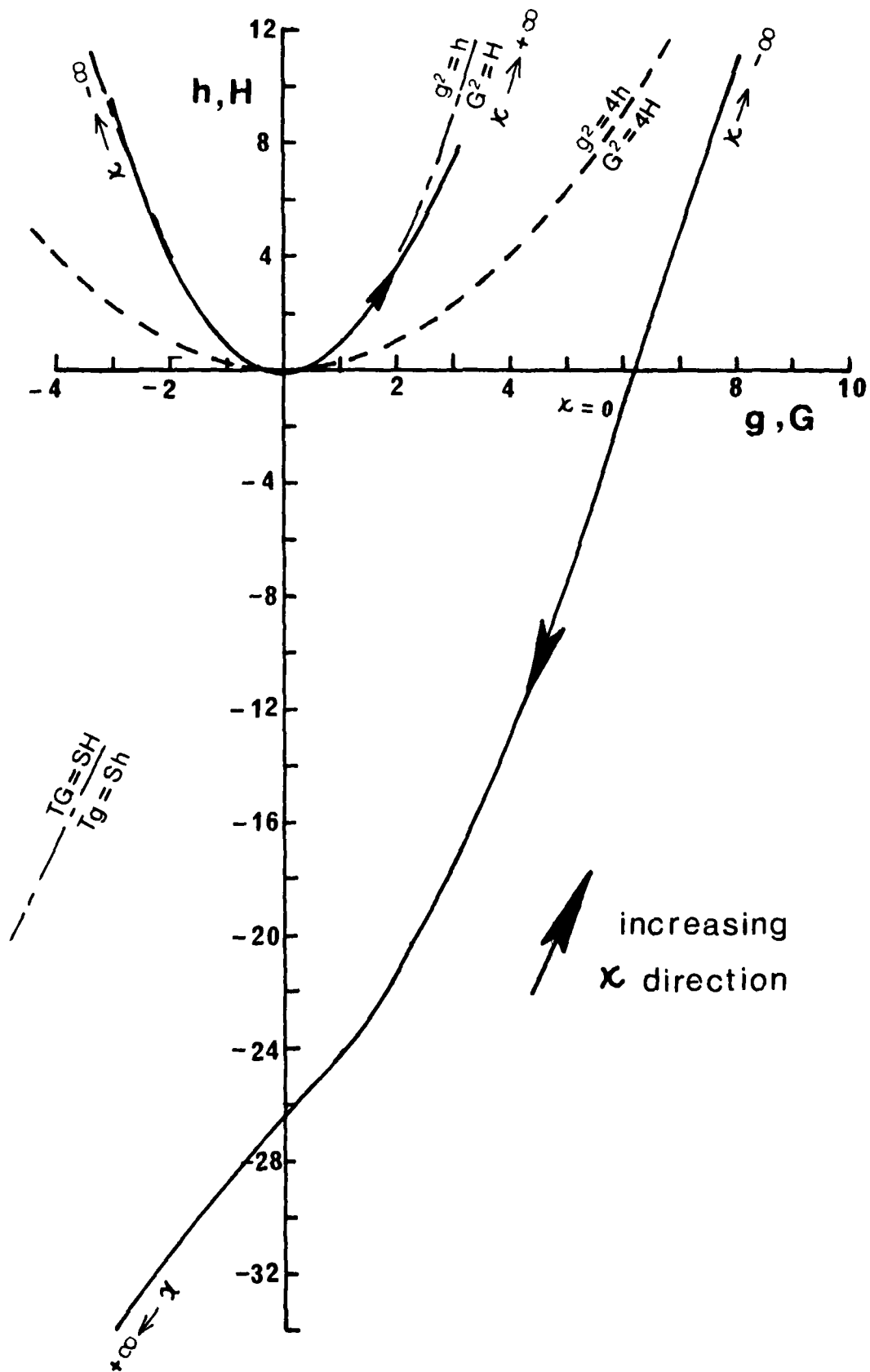


Fig 12 Loci corresponding to the two factors of the stability quartic (Spitfire V,  $H_m = -0.005$ )

Fig 13a&b

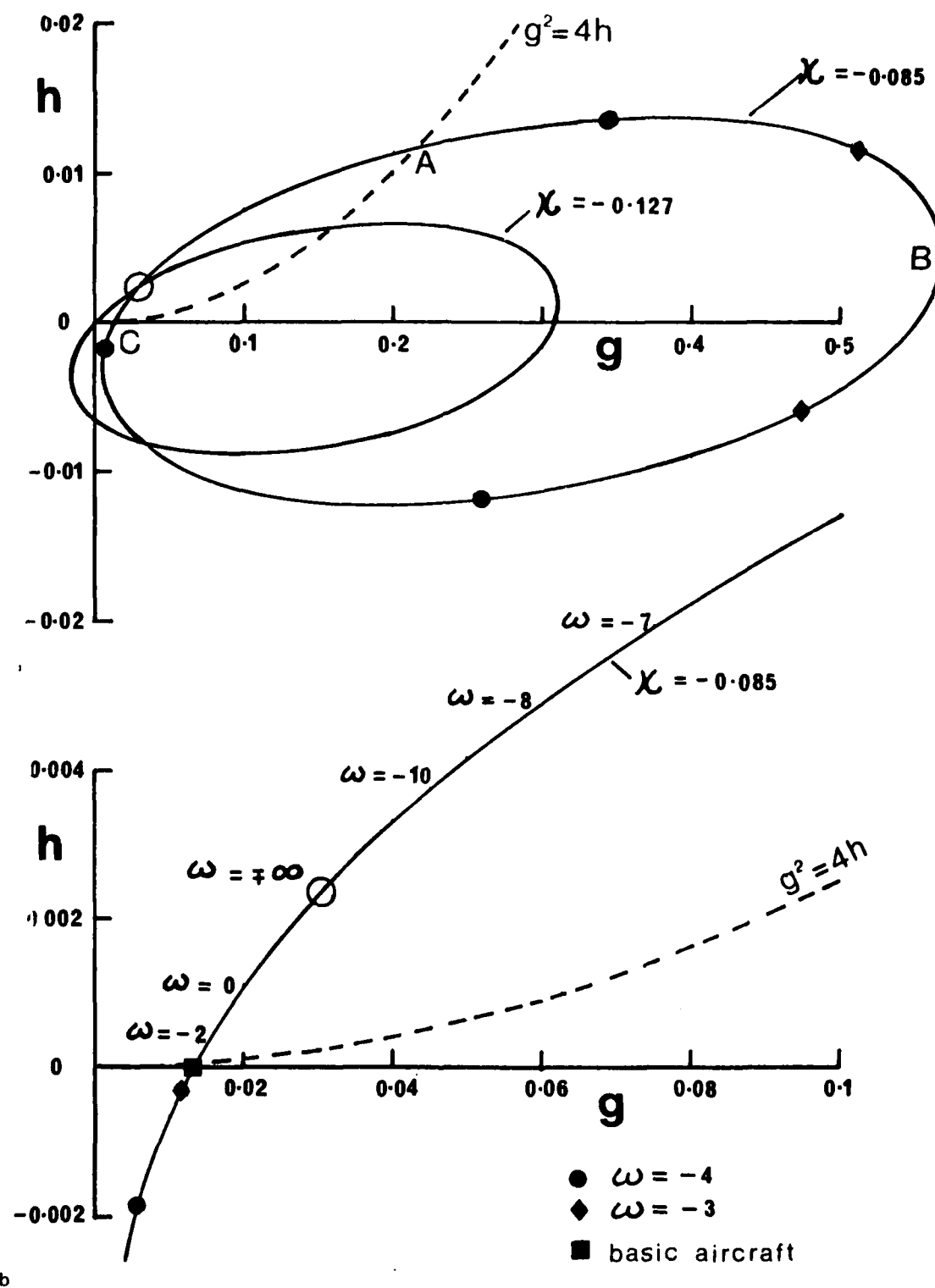


Fig 13a&b The  $g, h$  locus for varying  $\omega$  and fixed  $\kappa$  (Spitfire V) showing multiple points which occur for  $\omega = -3$  and  $-4$



Fig 14

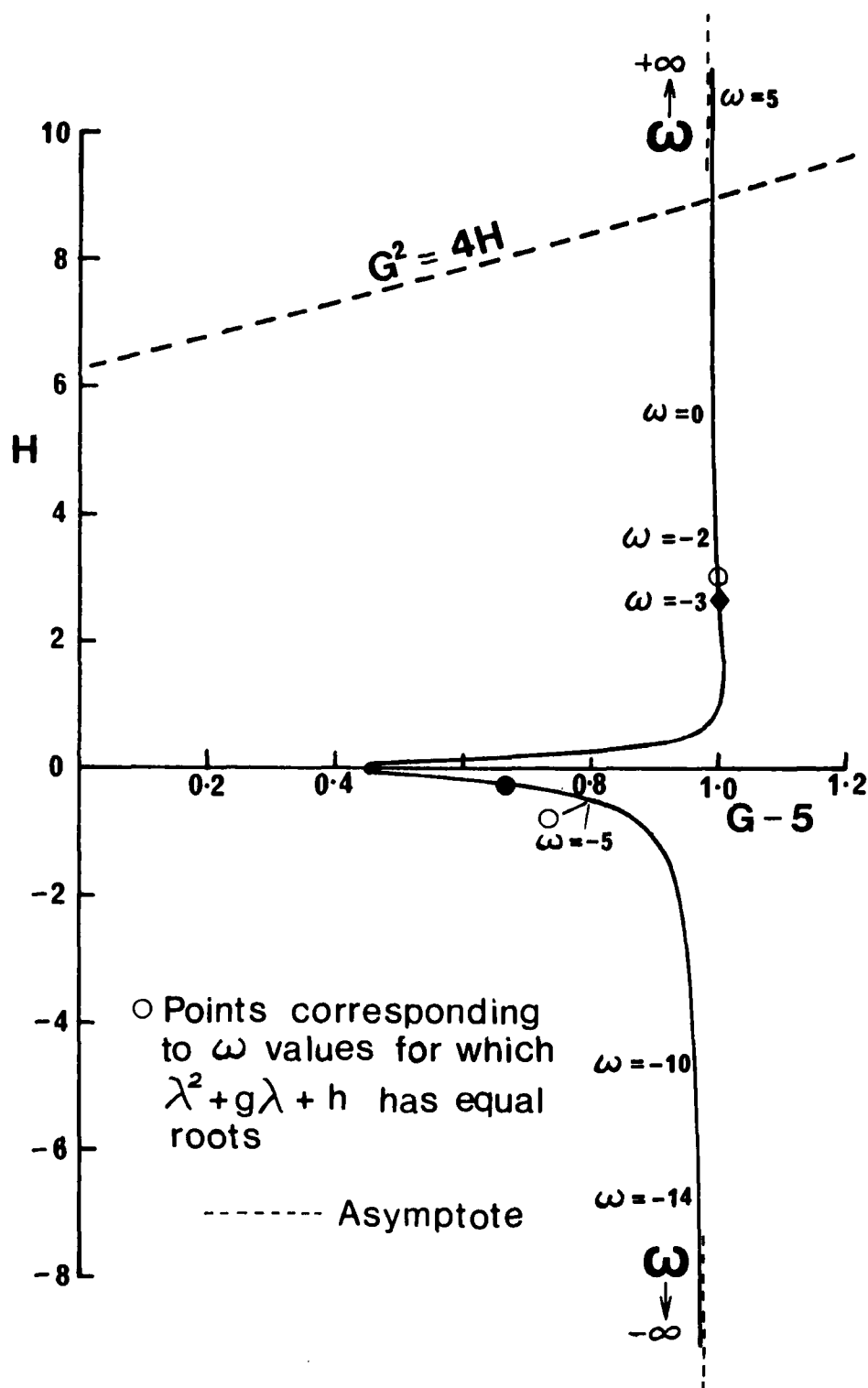


Fig 14 The locus of  $G, H$  for varying  $\omega$  ( $\kappa = -0.085$ ) associated with  $g, h$  locus of Fig 13 (Spitfire V)

Fig 15

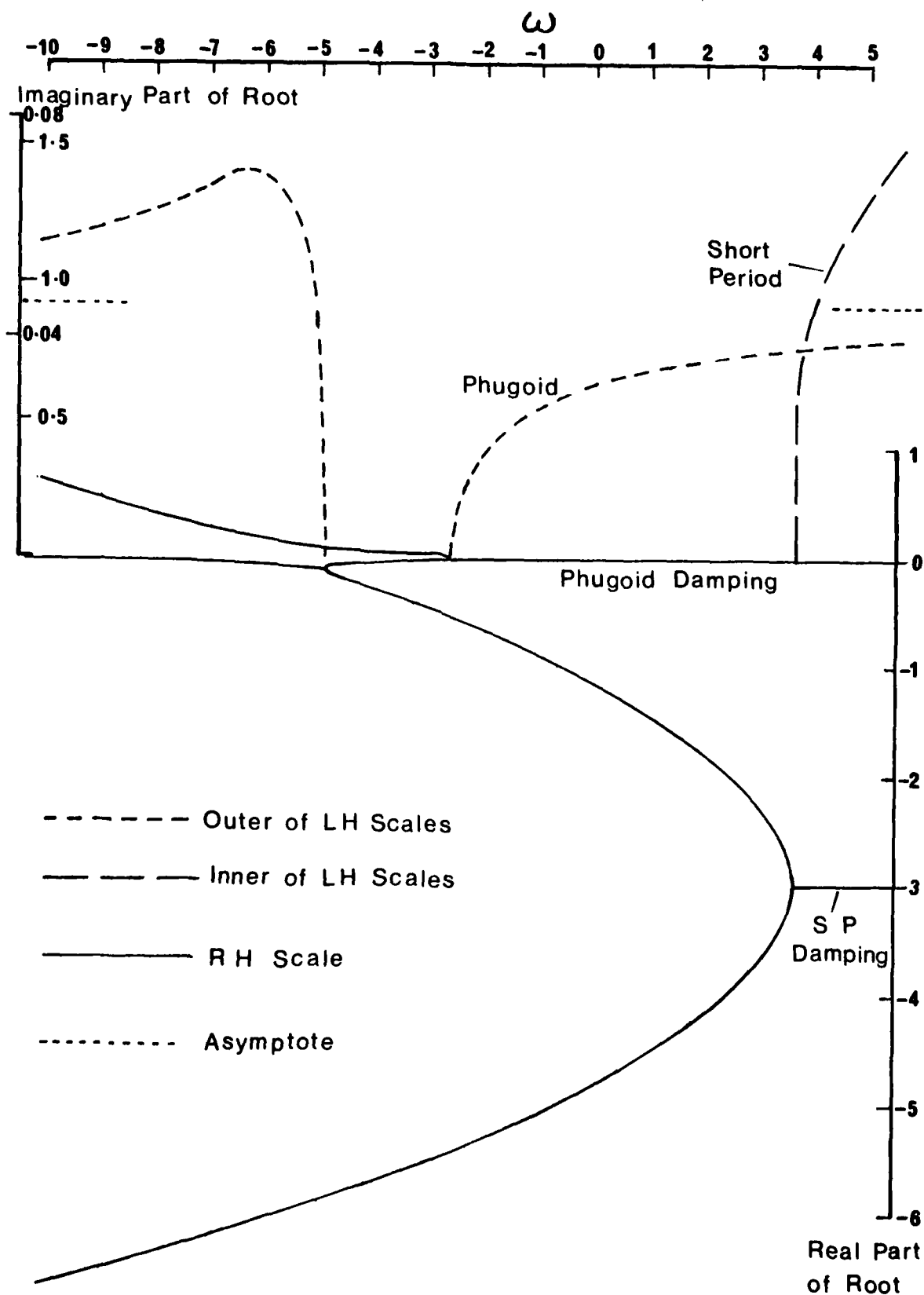


Fig 15 A one-parameter stability diagram constructed from the results of Figs 13 and 14

Fig 16

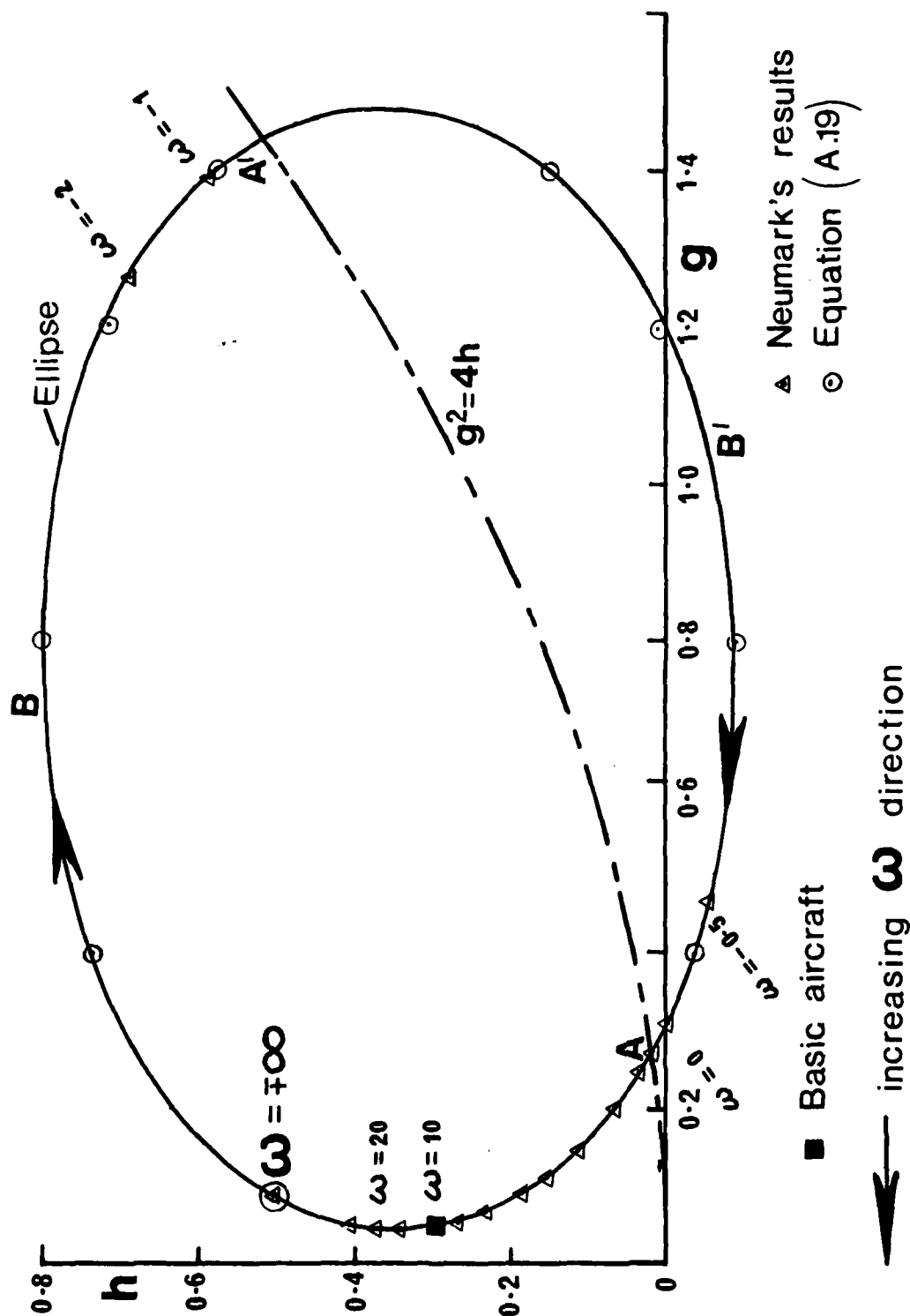


Fig 16 Locus of  $g, h$  for varying  $\omega$  (aircraft of Ref 7) with comparison of results obtained by present method and solution of quartic

Fig 17

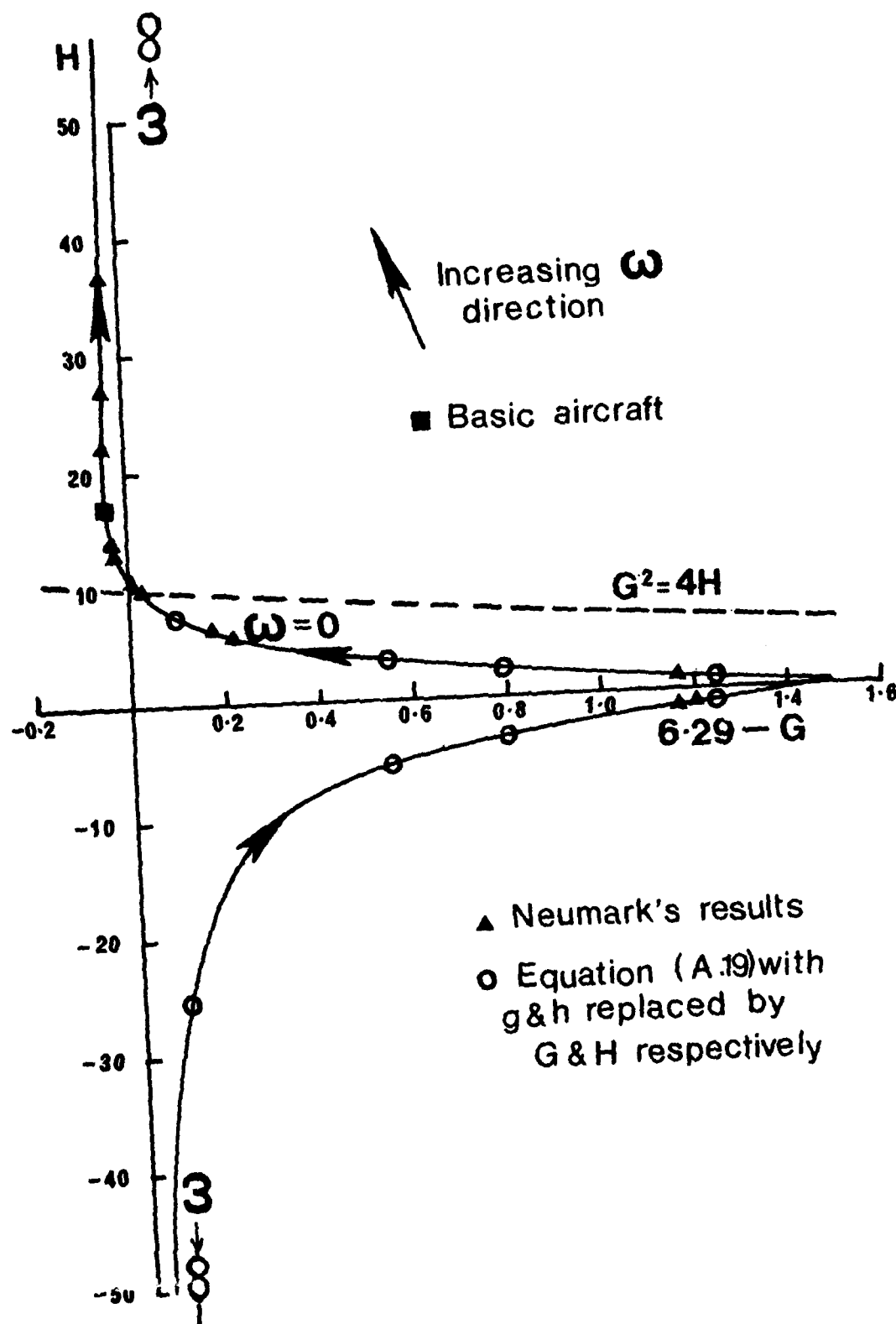


Fig 17 The  $G, H$  locus associated with that of Fig 16 including comparison of present results and those of Ref 7

Fig 18

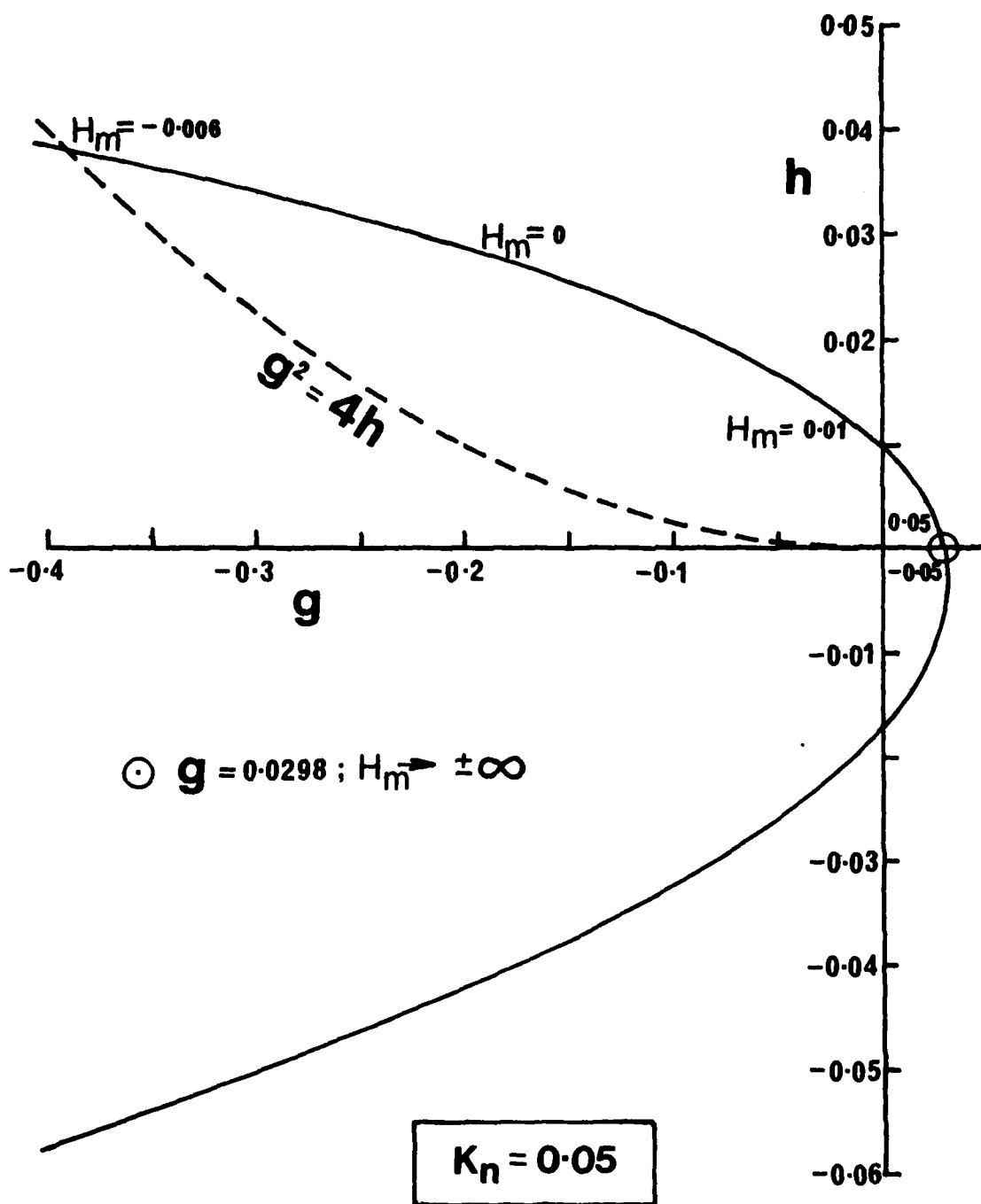


Fig 18 Locus of  $g, h$  for varying manoeuvre margin and fixed static margin (Spitfire V)

Fig 19

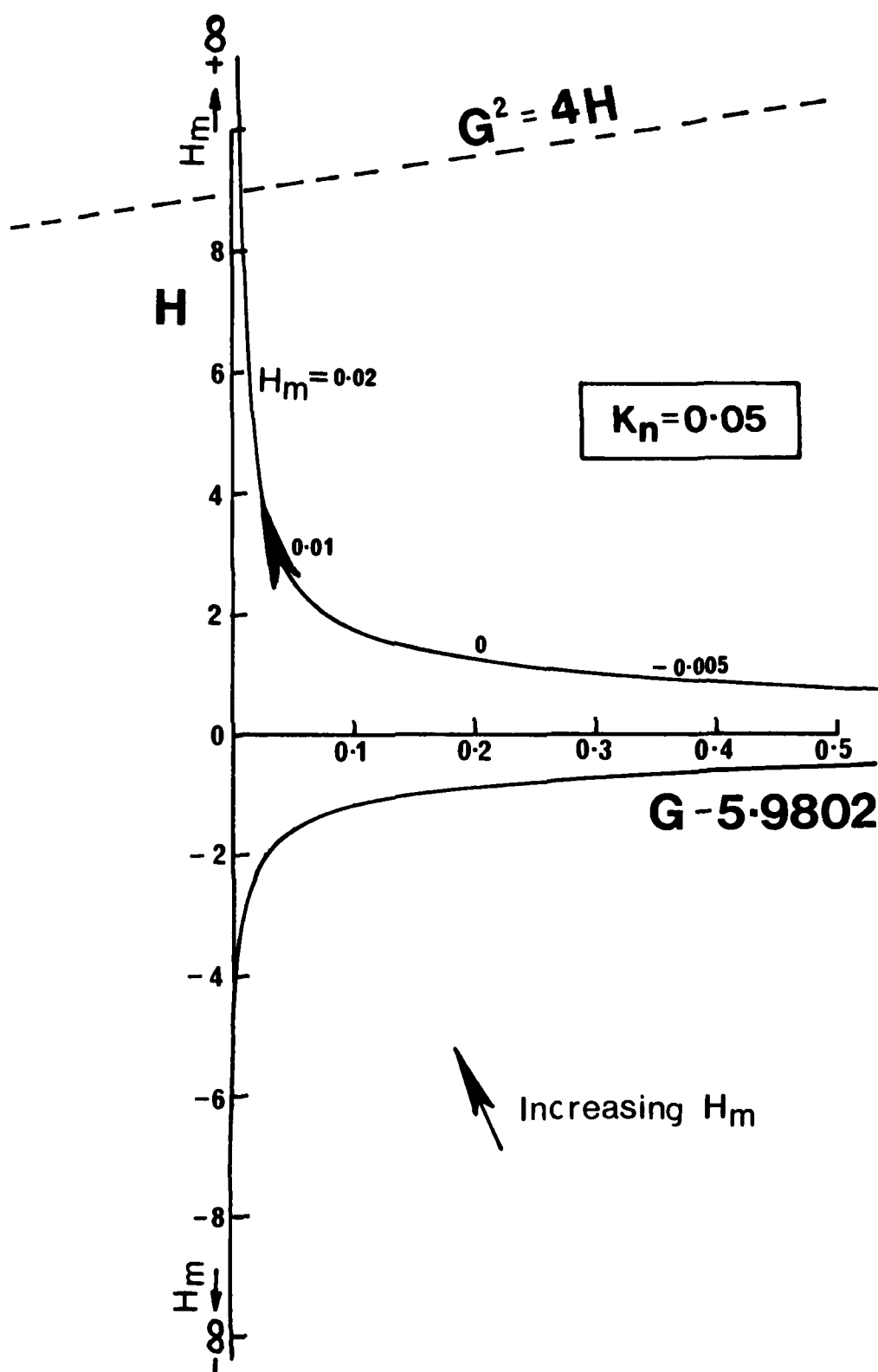


Fig 19 Locus of  $G, H$  associated with that of Fig 18 for varying manoeuvre margin and fixed static margin (Spitfire V)

Fig 20

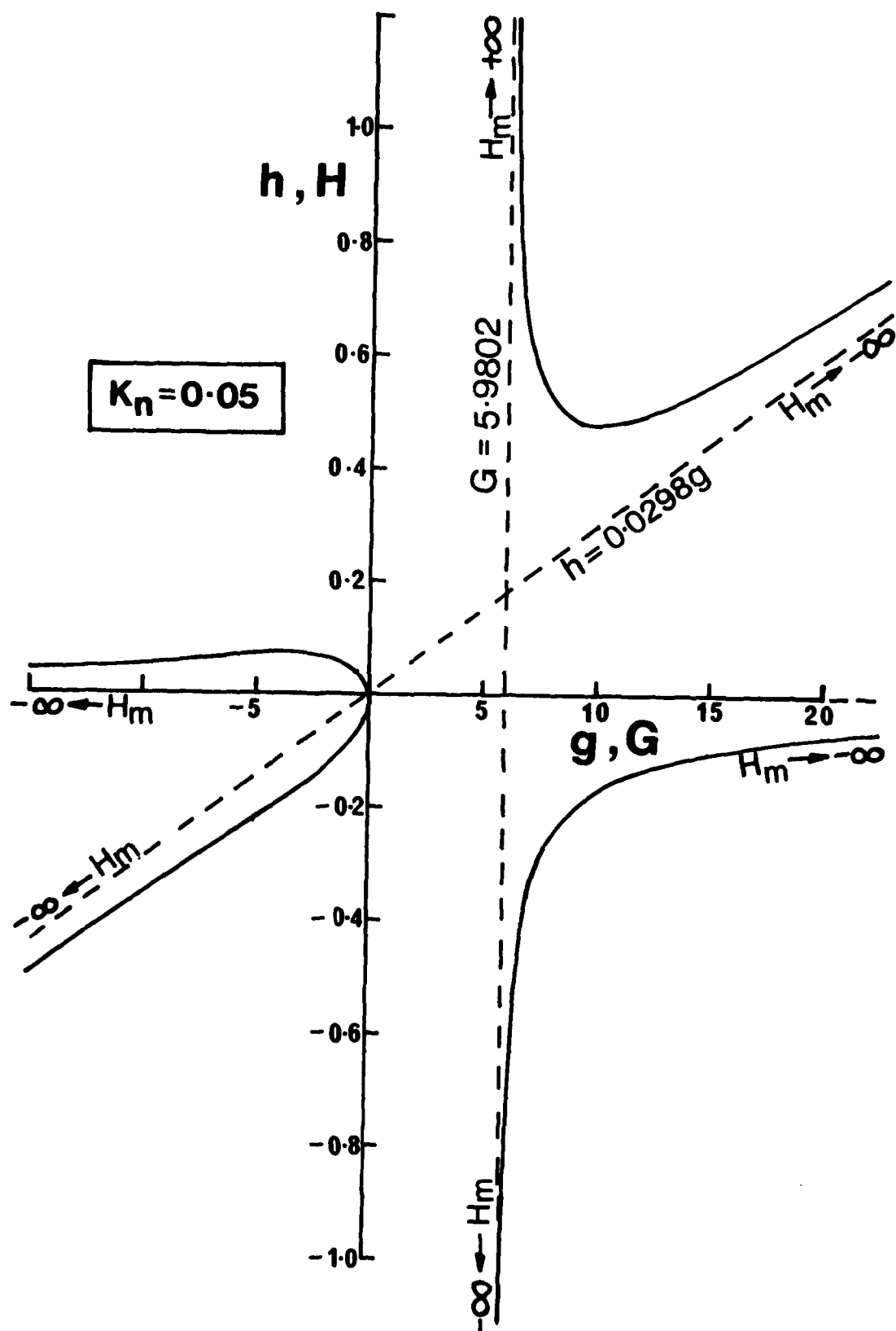


Fig 20 The loci of Figs 18 and 19 over the full range of  $H_m$  values

# REPORT DOCUMENTATION PAGE

Overall security classification of this page

UNLIMITED

As far as possible this page should contain only unclassified information. If it is necessary to enter classified information, the box above must be marked to indicate the classification, e.g. Restricted, Confidential or Secret.

1. DRIC Reference (to be added by DRIC)	2. Originator's Reference RAE TR 79065	3. Agency Reference N/A	4. Report Security Classification/Marking UNLIMITED		
5. DRIC Code for Originator 7673000W		6. Originator (Corporate Author) Name and Location Royal Aircraft Establishment, Farnborough, Hants, UK			
5a. Sponsoring Agency's Code N/A		6a. Sponsoring Agency (Contract Authority) Name and Location N/A			
7. Title On the use in stability analysis of the relationships between the coefficients of a quartic equation and those of a quadratic factor					
7a. (For Translations) Title in Foreign Language					
7b. (For Conference Papers) Title, Place and Date of Conference					
8. Author 1. Surname, Initials Thomas, H.H.B.M.	9a. Author 2 -	9b. Authors 3, 4 .... -	10. Date June 1979	Pages	Refs. 11
11. Contract Number N/A	12. Period N/A	13. Project	14. Other Reference Nos. Aero 3456		
15. Distribution statement (a) Controlled by - DRPC via DRIC (b) Special limitations (if any) -					
16. Descriptors (Keywords) (Descriptors marked * are selected from TEST) Stability of aircraft.					
17. Abstract <p>The stability of the perturbed longitudinal motion of an unaugmented aircraft about a given trimmed flight condition is determined by the well-known stability quartic. It is shown that two basic relationships exist between the coefficients of the quartic and those of a quadratic factor. It is possible to use the relationships to derive a further equation connecting the two coefficients of the quadratic factor as a single stability parameter is varied, all others being held constant.</p> <p>Examination of the position of the locus traced out by the point defined by the coefficients of the quadratic in relation to the axes and the parabolic boundary (separating real and complex roots) enables the trends in the nature of the degree of stability of the mode or modes represented by the quadratic factor to be determined.</p> <p>The use of this (as far as is known, novel) method of analysing aircraft stability is illustrated by a number of examples.</p>					



END  
THE  
FILMED  
8/8/00  
DTIC



AD-A085 864

ROYAL AIRCRAFT ESTABLISHMENT FARNBOROUGH (ENGLAND)  
ON THE USE IN STABILITY ANALYSIS OF THE RELATIONSHIPS BETWEEN T-ETC(U)  
JUN 79 H H THOMAS

F/G 1/1

UNCLASSIFIED

RAE-TR-79065

DRIC-BR-70237

NL

2-2

ALL INFORMATION  
7-81

SECURITY

INFORMATION

END

DATE

FILED

7-81

DTIC

**SUPPLEMENTARY**

**INFORMATION**

UDC 533.6.013.4 : 512.393 : 517.912.2

ROYAL AIRCRAFT ESTABLISHMENT

Corrigenda to Technical Report 79065

Received for printing 16 March 1981

ON THE USE IN STABILITY ANALYSIS OF THE RELATIONSHIPS BETWEEN THE COEFFICIENTS  
OF A QUARTIC EQUATION AND THOSE OF A QUADRATIC FACTOR

by

H. H. B. M. Thomas

CORRIGENDA

Page 4, section 2, line 1: R & M 3562 is Ref 10.

Pages 9 and 10, section 3.1: The equations in this section should contain the factor  $(K_2 - k_2)$  not  $(K_3 - k_2)$  as printed.

Page 13, section 5: The table of aircraft characteristics given at the foot of page 13 and top of page 14 is incorrect. It should read as follows:

$\mu_1$	=	272.155
$i_y$	=	1.75
$C_{Le}$	=	0.25
$x_u$	=	0.0376
$z_u$	=	0.50
$x_w$	=	- 0.139
$z_w$	=	4.899
$m_w$	=	113.839
$m_w^*$	=	1.200
$m_q$	=	6.543
$g$	=	$C_{Le}$

Page 14, penultimate paragraph of section 5 is incomplete. It should be amended to read:

"... becoming divergent, when condition (i) of page 10 is fulfilled. If condition (iii) applies increase of  $m_u$  achieves the same result."

Page 14, last sentence of section 5: The value of  $g$  quoted should be 0.06.

A more complete version of Fig 4 is attached. This corrects the value of  $m_w$  from 50 to 15 and inserts additional values along the curve.

Fig 4

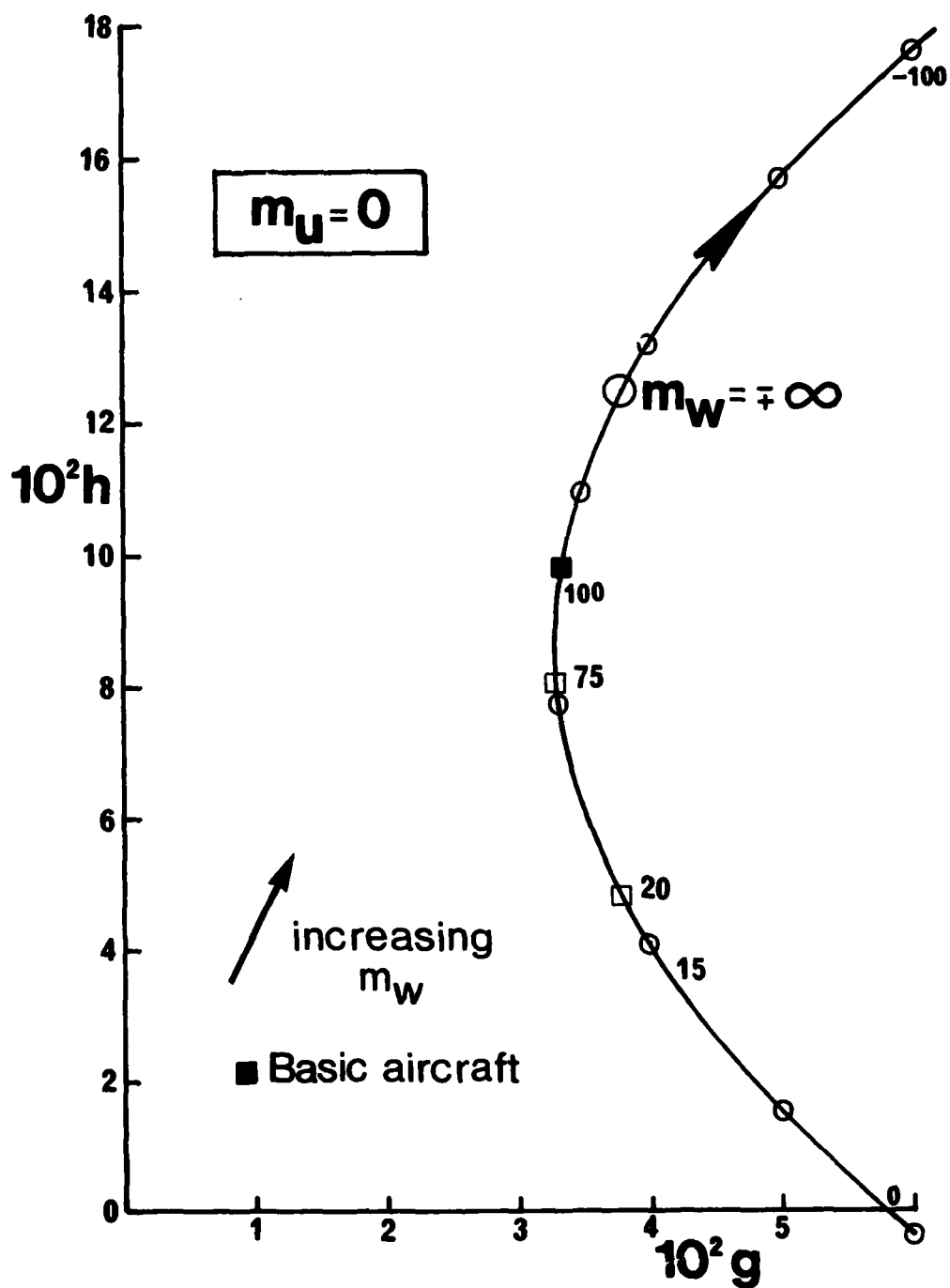


Fig 4 The locus of  $g, h$  as  $m_w$  is varied for the example aircraft of section 5